



1 **Coccolithophore biodiversity controls carbonate export in the Southern Ocean**

2 Andrés S. Rigual Hernández^{1,*}, Thomas W. Trull^{2,3}, Scott D. Nodder⁴, José A. Flores¹,
3 Helen Bostock^{4,5}, Fátima Abrantes^{6,7}, Ruth S. Eriksen^{2,8}, Francisco J. Sierro¹, Diana M.
4 Davies^{2,3}, Anne-Marie Ballegeer⁹, Miguel A. Fuertes⁹, and Lisa C. Northcote⁴.

5 1 Área de Paleontología, Departamento de Geología, Universidad de Salamanca, 37008
6 Salamanca, Spain

7 2 CSIRO Oceans and Atmosphere Flagship, Hobart, Tasmania 7001, Australia

8 3 Antarctic Climate and Ecosystems Cooperative Research Centre, University of
9 Tasmania, Hobart, Tasmania 7001, Australia

10 4 National Institute of Water and Atmospheric Research, Wellington 6021, New Zealand

11 5 University of Queensland, Brisbane, Queensland 4072, Australia

12 6 Portuguese Institute for Sea and Atmosphere (IPMA), Divisão de Geologia Marinha
13 (DivGM), Rua Alferedo Magalhães Ramalho 6, Lisboa, Portugal

14 7 CCMAR, Centro de Ciências do Mar, Universidade do Algarve, Campus de Gambelas,
15 8005-139 Faro, Portugal

16 8 Institute for Marine and Antarctic Studies, University of Tasmania, Private Bag 129,
17 Hobart, Tasmania 7001, Australia

18 9 Departamento de Didáctica de las Matemáticas y de las Ciencias Experimentales,
19 Universidad de Salamanca, 37008 Salamanca, Spain.

20 * Corresponding author

21 **Abstract**

22 Southern Ocean waters are projected to undergo profound changes in their
23 physical and chemical properties in the coming decades. Coccolithophore blooms in the
24 Southern Ocean are thought to account for a major fraction of the global marine calcium
25 carbonate (CaCO₃) production and export to the deep sea. Therefore, changes in the
26 composition and abundance of Southern Ocean coccolithophore populations are likely to
27 alter the marine carbon cycle, with feedbacks to the rate of global climate change.
28 However, the contribution of coccolithophores to CaCO₃ export in the Southern Ocean is
29 uncertain, particularly in the circumpolar Subantarctic Zone that represents about half of
30 the areal extent of the Southern Ocean and where coccolithophores are most abundant.
31 Here, we present measurements of annual CaCO₃ flux and quantitatively partition them
32 amongst coccolithophore species and heterotrophic calcifiers at two sites representative



33 of a large portion of the Subantarctic Zone. We find that coccolithophores account for a
34 major fraction of the annual CaCO_3 export with highest contributions in waters with low
35 algal biomass accumulations. Notably, our analysis reveals that although *Emiliania*
36 *huxleyi* is an important vector for CaCO_3 export to the deep sea, less abundant but larger
37 species account for most of the annual coccolithophore CaCO_3 flux. This observation
38 contrasts with satellite remote sensing images that mostly reflect *E. huxleyi* blooms as a
39 result of its higher cell abundance and detachment of its relatively small liths. It appears
40 likely that the climate-induced migration of oceanic fronts will initially result in the
41 poleward expansion of large coccolithophore species increasing CaCO_3 production.
42 However, subantarctic coccolithophore populations will eventually diminish as
43 acidification overwhelms those changes. Overall, our analysis emphasizes the need for
44 species-centred studies to improve our ability to project future changes in phytoplankton
45 communities and their influence on marine biogeochemical cycles.

46

47 **1. Introduction**

48 The emissions of carbon dioxide (CO_2) into the atmosphere by anthropogenic
49 industrial activities over the past 200 years are inducing a wide range of alterations in the
50 marine environment (Pachauri et al., 2014). These include ocean warming, shallowing
51 of mixed layer depths, changes in nutrient supply to the photic zone, and decreasing
52 carbonate-ion concentrations and pH of the surface ocean, a process known as ocean
53 acidification (Rost and Riebesell, 2004; Stocker et al., 2014). In particular, ocean
54 acidification poses a major global-scale risk for marine calcifying organisms because the
55 decline in the saturation state of carbonate minerals in seawater makes the biological
56 precipitation of carbonate difficult and increases the dissolution rates of their shells or
57 skeletons (Gattuso and Hansson, 2011). Owing to their moderate alkalinity and cold
58 temperatures, Southern Ocean waters are projected to become undersaturated with respect
59 to aragonite no later than 2040 and to calcite by the end of the century (Cao and Caldeira,
60 2008; McNeil and Matear, 2008; Shadwick et al., 2013). Since such thresholds will be
61 reached sooner in polar regions, Southern Ocean ecosystems have been proposed as
62 bellwethers for prospective impacts of ocean acidification on marine organisms at mid
63 and low latitudes (Fabry et al., 2009).

64 Coccolithophores are a major component of phytoplankton communities in the
65 Southern Ocean, particularly in its northern-most province, the Subantarctic Zone, where



66 they often exhibit maximum abundances and diversity (e.g. Gravalosa et al., 2008;
67 Saavedra-Pellitero et al., 2014; Malinverno et al., 2015; Charalampopoulou et al., 2016).
68 Coccolithophores play an important and complex role in the Southern Ocean carbon cycle
69 (Salter et al., 2014). On the one hand, the production of calcite platelets (termed
70 coccoliths) decreases the alkalinity of surface waters thereby reducing the atmospheric
71 uptake of CO₂ from the atmosphere into the surface ocean. On the other hand, the
72 production of organic matter through photosynthesis, and its subsequent transport to
73 depth in settling particles, enhances carbon sequestration via the biological carbon pump
74 (Volk and Hoffert, 1985). Additionally, due to their high density and slow dissolution,
75 coccoliths act as an effective ballast for organic matter, increasing organic carbon
76 sequestration depths (Buitenhuis et al., 2001; Boyd and Trull, 2007; Ziveri et al., 2007).
77 Therefore, changes in the abundance, composition and distribution of coccolithophores
78 could have an extensive impact on ocean nutrient stoichiometry, carbon sequestration,
79 and nutrition for higher trophic levels in the Southern Ocean (Deppeler and Davidson,
80 2017).

81 The remoteness and vastness of the Southern Ocean, together with the inherent
82 temporal and spatial variability of pelagic ecosystems, hampers accurate characterization
83 and quantification of Southern Ocean phytoplankton communities. Advances in satellite
84 technology and modelling algorithms have allowed a circumpolar and year-round
85 coverage of the seasonal evolution of major phytoplankton functional groups within the
86 Southern Ocean (e.g. Alvain et al., 2013; Hopkins et al., 2015; Rousseaux and Gregg,
87 2015). In particular, satellite reflectance observations have been used to quantitatively
88 estimate coccolithophore Particulate Inorganic Carbon (PIC) concentrations throughout
89 the Southern Ocean. These satellite estimates suggest apparent high PIC values during
90 summer near the major Southern Ocean fronts attributed to coccolithophores (Balch et
91 al., 2011; Balch et al., 2016). This band of elevated reflectance and PIC that encircles the
92 entire Southern Ocean was termed the “Great Calcite Belt” by these authors. However,
93 recent research (Trull et al., 2018) indicates that satellite ocean-colour-based PIC
94 estimates could be unreliable, particularly in Antarctic waters where they erroneously
95 suggests high PIC abundances. Shipboard observations, on the other hand, provide a
96 detailed picture of phytoplankton community composition and structure, but are
97 dispersed, both temporally and geographically, and provide rather heterogenous data in
98 terms of taxonomic groups investigated, and the sampling scales and methodologies used



99 (e.g. Kopczynska et al., 2001; de Salas et al., 2011; Poulton et al., 2013; Patil et al., 2017,
100 among others). *In situ* year-round monitoring of key strategic regions is critically needed
101 to establish baselines of phytoplankton community composition and abundance and to
102 validate and improve ocean biogeochemical models (Rintoul et al., 2012). This
103 information is also essential if we are to detect possible climate-driven changes in the
104 structure of phytoplankton communities that could influence the efficiency of the
105 biological carbon pump, with consequent feedbacks to the rate of deep-water carbon
106 sequestration and global climate change (Le Quéré et al., 2007; Deppeler and Davidson,
107 2017).

108 Here, we document coccolithophore and carbonate particle fluxes collected over
109 a year by four sediment trap records deployed at two strategic locations of the Australia
110 and New Zealand sectors of the Southern Ocean considered representative of a large
111 portion of the SAZ. Our measurements provide coccolith mass estimates of the main
112 coccolithophore species and quantitatively partition annual carbonate fluxes amongst
113 coccolithophore species and heterotrophic calcifiers. We find that coccolithophores are a
114 major vector for CaCO₃ export out of the mixed layer and that the largest contribution to
115 CaCO₃ export is not from the most abundant species *Emiliana huxleyi* but rather from
116 larger coccolithophores species with substantially different physiological traits (e.g.
117 *Calcidiscus leptoporus*). Our results emphasize the urgent need for diagnostic fitness
118 response experiments on other coccolithophore species aside from *E. huxleyi* (e.g. Feng
119 et al., 2017) in order to be able to predict the impacts of anthropogenically
120 induced changes in Southern Ocean ecosystems and biological carbon uptake
121 mechanisms.

122

123 2. Material and methods

124

125 2.1 Oceanographic setting

126 The SAZ alone accounts for more than half of the Southern Ocean area (Orsi et
127 al., 1995) and represents a transitional boundary between the warm, oligotrophic waters
128 of the subtropical gyres to the north and the cold, silicate-rich waters south of the Polar
129 Front (PF). The SAZ is arguably the largest high nutrient, low chlorophyll (HNLC)
130 province in the world's ocean and is central to the linkages between the ocean–
131 atmosphere CO₂ exchange and climate. The deep winter convection in the SAZ, which



132 that exceeds 400 m, results in the formation of a high-oxygen water masses known as
133 Subantarctic Mode and Antarctic Intermediate Waters that connect the upper and lower
134 limbs of the global overturning circulation (Sloyan and Rintoul, 2001a, b). The formation
135 of these water masses are responsible for the sequestration of a large fraction of
136 anthropogenic CO₂ (Sabine et al., 2004), with an estimated 1 Gt C yr⁻¹ transported to
137 intermediate depths annually (Metzl et al., 1999). Macronutrient concentrations display
138 pronounced seasonal changes in the SAZ with fully replete levels during winter to
139 substantial depletion during summer, particularly for silicate (Dugdale et al., 1995;
140 Rintoul and Trull, 2001; Bowie et al., 2011). Phytoplankton community in the
141 subantarctic zone is dominated by pico- and nanoplankton including cyanobacteria,
142 coccolithophores and autotrophic flagellates with lower abundances of diatoms than polar
143 waters south the Polar Front (Chang and Gall, 1998; Kopczynska et al., 2001; de Salas et
144 al., 2011; Rigual-Hernández et al., 2015b; Eriksen et al., 2018).

145

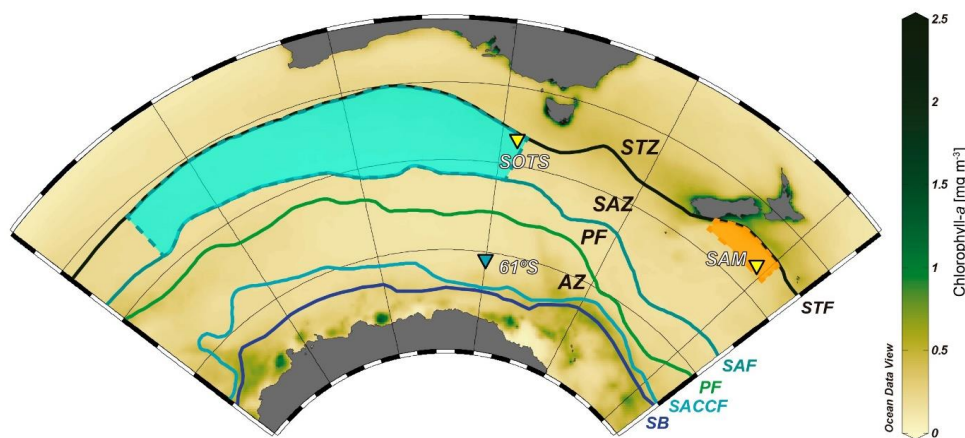
146 **2.2 Field experiments**

147 Here we report on the coccolithophore and biogeochemical fluxes collected over
148 a year at the Australian Southern Ocean Time Series (SOTS) observatory (Trull et al.,
149 2010) and the New Zealand Subantarctic Mooring (SAM) site (Nodder et al., 2016) (Fig.
150 1). The SOTS observatory is located in the abyssal plane of the central SAZ
151 approximately 530 km southwest of Tasmania (46° 56' S, 142° 15' E) within an anti-
152 cyclonic gyre in a region characterized by weak circulation (Trull et al., 2001; Herraiz-
153 Borreguero and Rintoul, 2011). SOTS was equipped with three vertically moored, conical
154 time-series sediment traps (McLane Parflux Mk 7G-21) placed at ~1000, 2000 and 3800
155 m depth between August 2011 until July 2012. The physical, chemical and biological
156 parameters of SOTS site are regarded as representative for large portion of the Indian and
157 Australian sectors of the SAZ (~90°E and 140°E; Trull et al., 2001). The SAM site is
158 located in the Bounty Trough in in the subantarctic waters south east of New Zealand
159 (46°40'S, 178° 30'E) and was equipped with conical, time-incremental sediment trap
160 (McLane PARFLUX Mk7G-21) placed at 1500 m depth, with samples used in the present
161 study collected between November 2009 until November 2010. The SAM site is
162 considered to be representative of a wide area of the northern sector of the SAZ off eastern
163 New Zealand, approximately 171°E to 179°W and 45 to 47°S (Law et al., 2014; Fig. 1).
164 Full details of the field experiments from these two localities in the Australian and New



165 Zealand sectors of the SAZ can be found in Trull et al. (2001) and Nodder et al. (2016),
166 respectively.

167



168

169 **Figure 1:** Chlorophyll-*a* composite map of the Australian-New Zealand sector of the
170 Southern Ocean (July 2002 to July 2012) from the MODIS Aqua Sensor showing the
171 location of the sediment trap moorings sites: SOTS, 61°S and SAM. The regions for
172 which the SOTS and SAM sites are representative are marked with light blue and orange
173 areas, respectively. Abbreviations: Subtropical front - STF, Subantarctic Zone – SAZ,
174 Subantarctic Front - SAF, Polar Frontal Zone - PFZ, Polar Front - PF, Antarctic Zone –
175 AZ, Southern Antarctic Circumpolar Current Front – SACCF, southern boundary of the
176 ACC – SB. Oceanic fronts after Orsi et al. (1995).

177 2.3 Sample processing

178 In short, the recovered trap bottles were refrigerated upon recovery and then
179 allowed to settle. The sample slurry was then wet-sieved through a 1 mm screen in the
180 case of SOTS (no attempt to extract zooplankton "swimmers" was made for the <1 mm
181 fraction analysed here) and through a 200 µm sieve to remove "swimmers" for the SAM
182 site. The remaining fraction was then split using a McLane wet sample divider; the SOTS
183 samples were subdivided into one tenth aliquots while one fifth splits were made for the
184 SAM samples. For the SOTS samples, a total of 55 samples were processed for calcareous
185 nannoplankton analysis. The one-tenth splits dedicated to phytoplankton analysis were
186 further subdivided into four aliquots with the McLane splitter. One aliquot was used for



187 calcareous nannoplankton analysis and the remaining three were kept refrigerated for
188 biomarker and non-calcareous microplankton analyses. In the case of the SAM samples,
189 the one-fifth aliquots were further subdivided into five subsplits, and one of those was
190 used for calcareous nannoplankton analysis. Two different types of glass slides per
191 sample were prepared. The first preparation was used for the estimation of coccosphere
192 and calcareous dinocyst (calcispheres of thoracosphaerids) fluxes and for coccolith
193 imaging. A volume ranging between 1000 and 5000 μl of the raw sample was mounted
194 on a glass slide using Canada balsam following Flores and Sierro (1997). This technique
195 produces random settling of the coccoliths for microscopic identification and
196 enumeration. The second type of glass slide was prepared following a modified protocol
197 for non-destructive disintegration of aggregates modified from Bairbakhish et al. (1999).
198 The objective of this chemical treatment is to reduce biases in the coccolith flux
199 estimations associated with the presence of different types of aggregates and
200 coccospheres (Bairbakhish et al., 1999). In brief, 2000 μl were extracted from the aliquot
201 for calcareous nannoplankton analysis and then treated with a solution comprising 900 μl
202 sodium carbonate and sodium hydrogen carbonate, 100 μl ammonia (25%) and 2000 μl
203 hydrogen peroxide (25%). The sample was agitated for 10 seconds every 10 minutes and
204 this process was repeated over an hour. Then, the reaction was stopped with catalase
205 enzyme and samples were allowed to settle for at least 48 hours before preparation on
206 microscope slides. pH controls indicate that the solution kept pH levels near 9, therefore
207 precluding coccolith dissolution. Finally, trap samples were mounted on microscope
208 slides following the same decantation method as used for the first type of glass slides (i.e.
209 Flores and Sierro, 1997).

210 **2.4 Determination of CaCO_3 fluxes**

211 A detailed description of the geochemical analytical procedures for the SOTS
212 samples is provided in Trull et al. (2001) and Rigual-Hernández et al. (2015a) while more
213 detailed procedures of the SAM trap can be found in Nodder et al. (2016). In short, for
214 the SOTS site three of the one tenth splits were filtered onto 0.45 pore size filters. Then
215 the material was removed from the filter as a wet cake of material, dried at 60°C, and
216 ground in an agate mortar. This material was used to determine the total mass and
217 composition of the major components of the flux. Particulate inorganic Carbon (PIC)
218 content was measured by closed system acidification with phosphoric acid and
219 coulometry. For the SAM site, one-fifth split was analysed for elemental calcium (Ca)



220 concentration using ICP-MS techniques. The samples were oven-dried, digested in
221 nitric/hydrochloric acid and then analysed according to the methods under US EPA 200.2.
222 Ca was used to estimate CaCO₃ content in the samples assuming a 1:1 molar ratio in
223 CaCO₃.

224

225

226 **2.5 Quantification and characterization of coccolithophore sinking assemblages**

227 Qualitative and quantitative analyses of coccospheres and coccoliths were
228 performed using a Nikon Eclipse 80i polarised light microscope at 1000 x magnification.
229 The taxonomic concepts of Young et al. (2003) and the Nannotax website (Young et al.,
230 2019) were used. A target of 100 coccospheres and 300 coccoliths was established;
231 however, owing to the pronounced seasonality in coccolithophore export, there were
232 some periods with very low abundance of coccospheres in the samples and therefore the
233 target of 100 coccospheres was not always met. Coccosphere and coccolith species counts
234 were then transformed into daily fluxes after Rigual Hernández et al. (2018).

235

236 **2.6 Determination of coccolith mass and size**

237 Birefringence and morphometric methods are the two most commonly used
238 approaches for estimating the calcite content of isolated coccoliths. The circularly-
239 polarized light-microscopy-based technique (Fuertes et al., 2014) is based on the
240 systematic relationship between the thickness of a given calcite particle (in the thickness
241 range of 0 - 1.55 μm) and the first-order polarization colours that it displays under
242 polarized light (Beaufort, 2005; Beaufort et al., 2014; Bolton et al., 2016). The advantages
243 of this approach are that: (i) it directly measures complete coccoliths with no assumptions
244 regarding their shape or thickness and (ii) it allows for quantification of calcite losses
245 associated with missing parts or etching of the coccoliths. Disadvantages of this technique
246 are the errors associated with the coccolith-calcite calibration and their consequent effect
247 on the coccolith mass estimates (Fuertes et al., 2014; González Lemos et al., 2018). The
248 morphometric approach, on the other hand, allows better taxonomic identification of the
249 coccoliths and has smaller errors in the length measurements (~0.1 to 0.2 μm; Poulton et
250 al. 2011). However, this method does not allow direct measurement of coccolith thickness
251 and assumes identical shape and width proportions for all specimens of the same species,
252 among other uncertainties (see Young and Ziveri, 2000 for a review). Since the two



253 methods have different associated errors (Poulton et al., 2011), we applied both
254 approaches to our coccolith flux data in order to obtain two independent estimates of the
255 fractional contribution of coccolithophores species to total carbonate export in the SAZ.

256 For the birefringence-based approach, a minimum of 50 coccoliths of each of the
257 main coccolithophore species were imaged using a Nikon Eclipse LV100 POL light
258 microscope equipped with circular polarisation and a digital camera (Nikon DS-Fi1 8-bit
259 colour). The only exception was *E. huxleyi* for which coccolith mass values had already
260 been estimated in all the same samples at high resolution by Rigual-Hernández et al.
261 (under review). For the minor components of the flux assemblage, a lower number of
262 coccoliths were measured (Table 1). A photograph of the same apical rhabdolith of the
263 genus *Acanthoica* was taken and used for calibration at the beginning of each imaging
264 session during which microscopy light and camera settings were kept constant. A
265 different number of fields of view of multiple samples representative of different seasons
266 were photographed until the target number of coccoliths for each species was reached.
267 Photographs were then analysed by the image processing software C-Calcita. The output
268 files for single coccoliths were visually selected and classified into the lowest possible
269 taxonomic level. Length and weight measurements were automatically determined by C-
270 Calcita software. Morphometric measurements of all the species are summarized in Table
271 1. For further methodological details see Fuertes et al. (2014) and Bolton et al. (2016).

272 The second approach consisted of performing morphometric measurements on the
273 coccoliths followed by the estimation of their coccolith mass assuming a systematic
274 relation between length and thickness (Young and Ziveri, 2000). Young and Ziveri (2000)
275 proposed that the calcite content of a given coccolith could be estimated using the
276 following formula:

$$277 \text{Coccolith calcite (pg)} = 2.7 \times k_s \times l^3$$

278 where 2.7 is the density of calcite (CaCO_3 ; $\text{pg } \mu\text{m}^3$), “ k_s ” is a shape constant that varies
279 between species and morphotypes and whose value is based on the reconstruction of
280 coccolith cross profiles and “ l ” is the distal shield length (DSL). In order to undertake
281 coccolith measurements on the same coccoliths used for the birefringence-based
282 approach, we employed the distal shield length values measured by C-Calcita using
283 circularly polarized light instead of morphometric measurements on Scanning Electron
284 Micrographs (SEM) as made in Young and Ziveri (2000).



285 Since coccolith distal shield length (DSL) has been reported to be systematically
286 underestimated using cross-polarized light microscopy (e.g. D’Amario et al., 2018), we
287 evaluated the possible errors in the DSL measurements made by C-Calcita. For this
288 assessment, we measured 40 detached coccoliths of *C. leptoporus* under the SEM from
289 samples of the SOTS sediment traps using the image processing software Image-J.
290 Average DSL measurements under the SEM were then compared with those made by C-
291 Calcita on 40 randomly selected *C. leptoporus* coccoliths. The average coccolith length
292 obtained with the SEM analysis (6.37 ± 1.02 , $n = 40$) was ~ 4% shorter than that estimated
293 with C-Calcita (6.62 ± 1.47 , $n = 40$). Therefore, we assumed the error for the DSL
294 measurements with circularly polarized light is < 5%. For the k_s value of each taxa, data
295 from the literature were (Table 1). *E. huxleyi* assemblages in the SAZ are composed of a
296 mixture of five different morphotypes: A, A overcalcified, B, B/C and C, each of which
297 is characterized by different shape factors (k_s). Since k_s is not available for all the
298 morphotypes found in the SAZ and it is not possible to differentiate between morphotypes
299 in our light microscopy images, we used the mean shape factor constant for *E. huxleyi*
300 (i.e. $k_s = 0.0275$) to provide a range of coccolith mass estimates for this species (Table 1
301 and Fig. 4).

302 2.7 Calculation of annual estimates

303 Since the trap collection periods encompassed a period shorter than a calendar
304 year, annual estimates of coccolith and CaCO_3 fluxes had to be estimated. For the SOTS
305 site, a total of 336 days were sampled for the 1000 and 2000 m traps and 338 days for the
306 3800 m. Since the unobserved interval occurred in winter, the missing sampling period
307 was filled using an average flux value of the winter cups (first and last trap bottles). In
308 the case of the SAM trap, the number of samples available for CaCO_3 and calcareous
309 nannoplankton analyses was different, covering a period of 313 and 191 days
310 respectively. Since gaps were quasi-equally distributed along the time series, annual
311 fluxes were estimated by filling the gaps in the record with average fluxes calculated from
312 the available data. The estimated range of the annual contribution of coccolithophores to
313 total CaCO_3 export at the SOTS and SAM traps was calculated by multiplying the
314 coccolith flux of each species in each sampling interval by its average coccolith weight
315 values obtained with the birefringence and morphometric techniques.

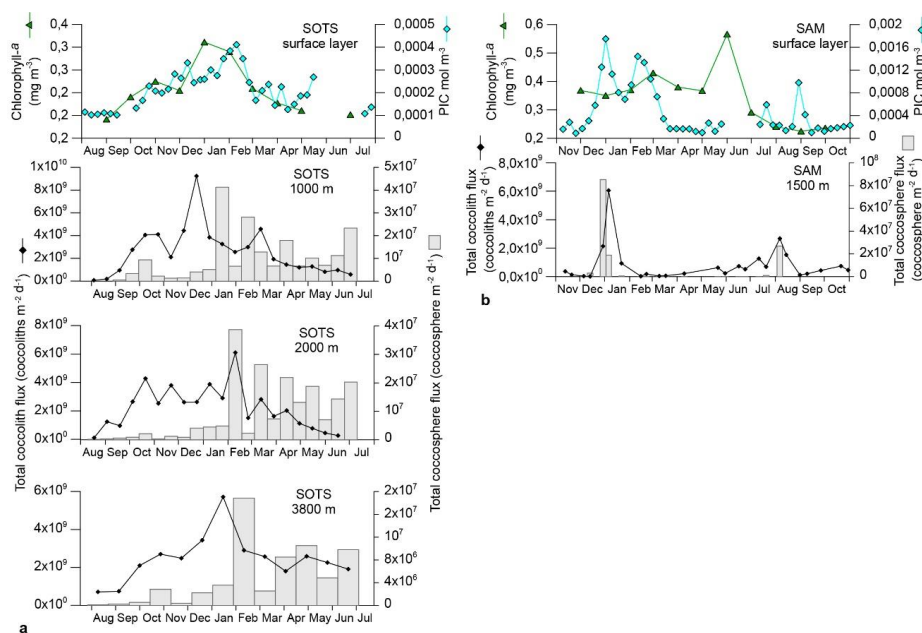
316 3. RESULTS



317 **3.1 Magnitude and seasonality of coccolithophore fluxes**

318 Annualized coccolith fluxes were similar at the SOTS three trap depths, with 8.6,
319 7.3 and 8.6×10^{11} liths $\text{m}^{-2} \text{yr}^{-1}$ at 1000, 2000 and 3800 m respectively, and about three
320 times larger than those of the SAM site (3.0×10^{11} liths $\text{m}^{-2} \text{yr}^{-1}$). The contribution of
321 intact coccospheres to the total coccolith export was low at both sites, with annual
322 coccosphere fluxes two orders of magnitude lower than coccolith fluxes at SOTS (3.5,
323 3.3 and 1.8×10^9 coccospheres $\text{m}^{-2} \text{yr}^{-1}$ at 1000, 2000 and 3800 m, respectively) and SAM
324 (2.2×10^9 coccospheres $\text{m}^{-2} \text{yr}^{-1}$).

325 Both coccolith and coccosphere fluxes displayed a marked seasonality that
326 followed the general trend of algal biomass accumulation in the surface waters at the
327 SOTS and SAM sites (Fig. 2). Coccolith fluxes at 1000 m started to increase in early
328 October and remained above the threshold of 1×10^9 coccoliths $\text{m}^2 \text{d}^{-1}$ until mid-April,
329 i.e. approximately eight months (Fig. 2). Three maxima were recorded during the period
330 of high coccolith export: October-early November 2011 (4×10^9 coccoliths $\text{m}^2 \text{d}^{-1}$), late
331 December 2011 (9×10^9 coccoliths $\text{m}^2 \text{d}^{-1}$) and March 2012 (4×10^9 coccoliths $\text{m}^2 \text{d}^{-1}$).
332 Coccolith fluxes of the main coccolithophore species generally followed the similar
333 seasonal pattern to that of the total coccolith flux (Supplementary figure 1) and are not
334 discussed further. Coccolithophore fluxes registered by the 2000 and 3800 m sediment
335 traps followed a generally similar seasonal pattern to those of the shallower trap at the
336 SOTS site (Fig. 2). At SAM, coccolith fluxes exhibited a strong seasonality with peak
337 fluxes in early January 2010 (up to 6×10^9 coccoliths $\text{m}^2 \text{d}^{-1}$) and a secondary peak in
338 August 2010 (3×10^9 coccoliths $\text{m}^2 \text{d}^{-1}$). Coccosphere fluxes at both sites displayed
339 maximum fluxes during the austral summer and minima during winter; however
340 maximum coccosphere export peaks did not always match those of coccolith export (Fig.
341 2).



342 a

343 **Figure 2:** Satellite-derived chlorophyll-*a* and Particulate Inorganic Carbon (PIC)
 344 concentration in the surface layer and total coccolith and coccosphere fluxes registered
 345 by the sediment traps at the SOTS (a), SAM (b) and 61°S sites (c, Rigual Hernández et
 346 al., 2018). Coccosphere fluxes are not available for the 61°S site.

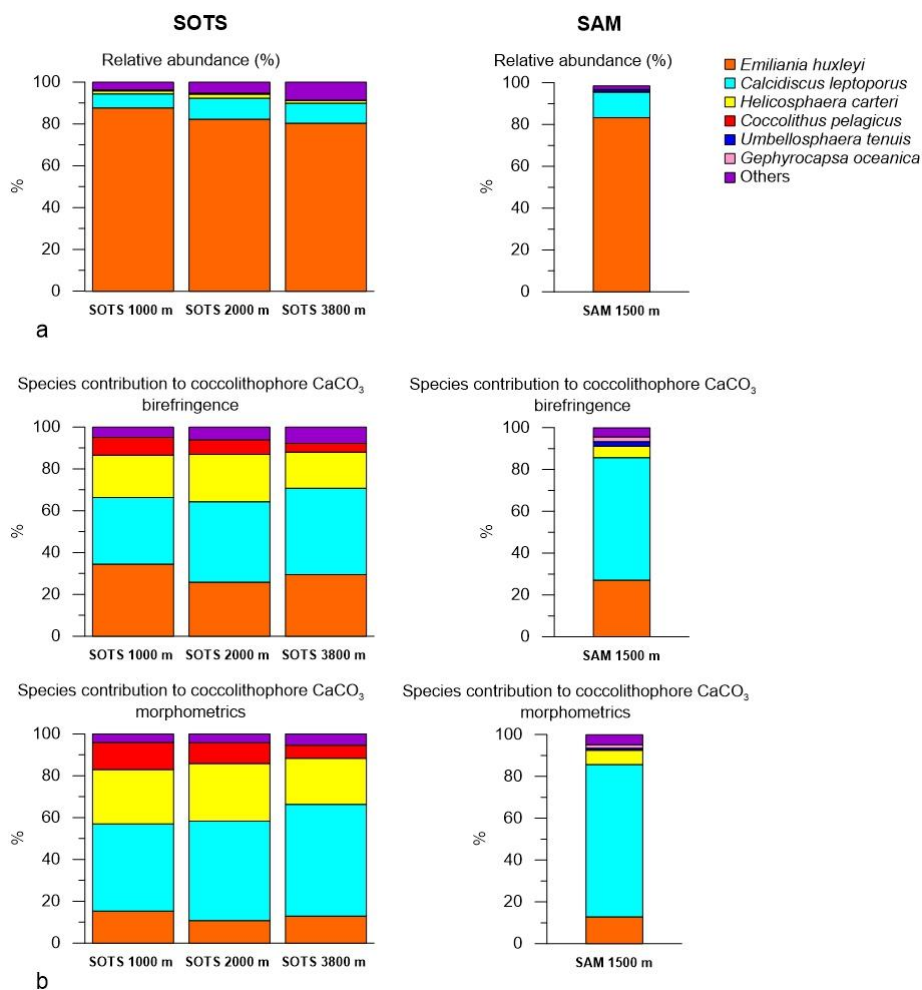
347 3.2. Coccolithophore assemblage composition

348 Coccolith sinking assemblages were overwhelmingly dominated by *Emiliania*
 349 *huxleyi* for all sediment trap records analysed (Fig. 3a). At the SOTS site, the annualized
 350 integrated relative contribution of *E. huxleyi* decreased slightly with depth, comprising
 351 88% of the total coccolithophore assemblage at 1000 m, 82% at 2000 m and 80% at 3800
 352 m. Secondary components of the coccolith sinking assemblage were *Calcidiscus*
 353 *leptoporus* (*sensu lato*) (6.7, 10.2 and 9.7% at 1000, 2000 and 3900 m, respectively),
 354 *Helicosphaera carteri* (1.4, 2 and 1.4%) and small *Gephyrocapsa* spp. (< 3 μm) (1.4, 1.5
 355 and 4.4%). Background concentrations (≤ 1%) of *Calciosolenia* spp., *Coccolithus*
 356 *pelagicus*, *Gephyrocapsa muelleriae*, *Gephyrocapsa oceanica*, *Gephyrocapsa* spp. (> 3
 357 μm), *Syracosphaera pulchra*, *Syracosphaera* spp., *Umbellosphaera tenuis* (*sensu lato*),
 358 and *Umbilicosphaera sibogae* were also registered. At the SAM site, *E. huxleyi* accounted
 359 for 83% of the annualized coccolith flux, with subordinate contributions of *C. leptoporus*
 360 (12.2%) and *Gephyrocapsa* spp. (< 3 μm) (1.5%). Background concentrations (< 1%) of



361 *Calciosolenia* spp., *G. oceanica*, *Gephyrocapsa* spp. (> 3 μm), *H. carteri*, *Syracosphaera*
 362 spp., *U. sibogae* and *U. tenuis* were observed.

363



364 **Figure 3:** a. Annualized integrated relative abundance of the most important
 365 coccolithophore species in the SOTS and SAM sediment trap records. b. Fractional
 366 contribution of coccolithophore species to total coccolithophore CaCO₃ in the SOTS and
 367 SAM sediment traps.

368 3.3 Calcite content per species

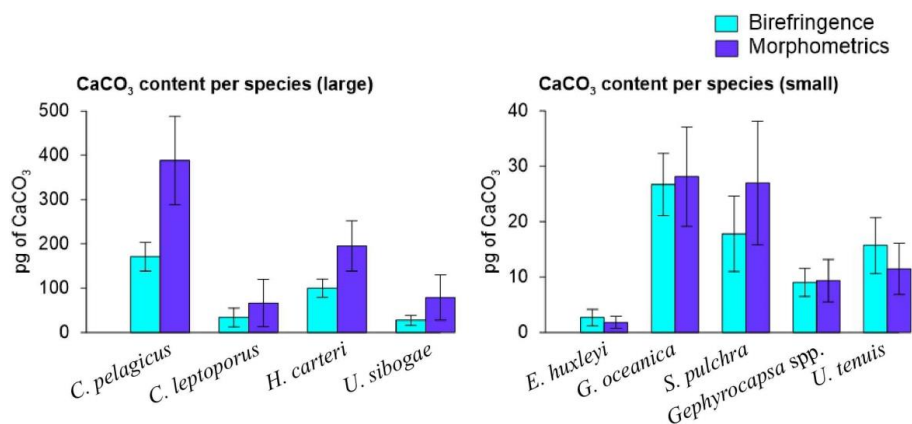
369 Coccolith length and mass for all species measured using birefringence and
 370 morphometric techniques are provided in Table 1. Overall, the average coccolith mass
 371 estimates for the coccolithophore species at SOTS and SAM sites using both approaches



372 are within the range of values in the published literature. The Noelaerhabdaceae family
 373 members, *G. oceanica* and *Gephyrocapsa* spp., display almost identical mass values with
 374 both approaches (Fig. 4). In contrast, substantial discrepancies are identifiable for *C.*
 375 *pelagicus*, *C. leptoporus*, *H. carteri* and *U. sibogae*, for which coccolith mass estimates
 376 are about two-fold greater using morphometrics than with the birefringence approach.
 377 The range of annual contributions of coccolithophores to carbonate is illustrated in Figure
 378 5.

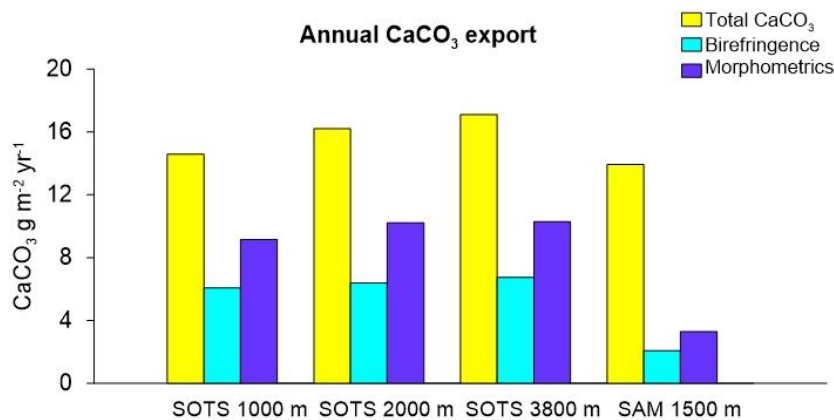
Species and morphotypes	Type of measurement	n	Length (µm)		Mass CaCO ₃ (pg)		k _s	Crystal units types	References
			Average	SD	Average	SD			
<i>Calcidiscus leptoporus</i>	Birefringence	210	6.39	1.49	33.65	21.11	-	V and R	
	Morphometrics	210	6.39	1.49	66.23	53.28	0.080		1
	Literature estimates	-	4.3-9.6		22.6-125.2		0.061-0.105		1.2
<i>Coccolithus pelagicus</i>	Birefringence	54	13.28	1.14	170.90	32.33	-	V and R	
	Morphometrics	54	13.28	1.14	387.96	99.64	0.060		1
	Literature estimates	-	8.5-13.5		99.5-398.6		0.051 - 0.060		1.2,3
<i>Emiliana huxleyi</i>	Birefringence	12842	2.78	0.57	2.64	1.43	-	R	
	Morphometrics	12842	2.78	0.57	0.99-2.64 (1.81)*	0.60-1.60	0.015-0.04 (0.0275)*	(V-unit vestigial)	
<i>E. huxleyi</i> type A	Literature estimates	-	3-4		1.50 - 3.50		0.02		1,4,5
<i>E. huxleyi</i> type A o/c	Literature estimates	-	3.5		4.6		0.04		1
<i>E. huxleyi</i> type B/C	Literature estimates	-	1.8-5.5		0.3-3.5		0.015		5,6,7
<i>E. huxleyi</i> type B	Literature estimates	-	3.5-5		2.30 - 6.81		0.02		1.5
<i>Gephyrocapsa oceanica</i>	Birefringence	51	5.87	0.62	26.70	5.64	-	R	
	Morphometrics	51	5.87	0.62	28.14	8.97	0.050	(V-unit vestigial)	
	Literature estimates	-	5-5.35		16.9-25.7		0.050-0.062		1.2
<i>Gephyrocapsa</i> spp.	Birefringence	10	4.03	0.59	9.00	2.51	-	R	
	Morphometrics	10	4.03	0.59	9.33	3.84	0.050	(V-unit vestigial)	1
	Literature estimates	-	-	-	-	-	-		
<i>Helicosphaera carteri</i>	Birefringence	64	11.20	1.12	100.10	20.34	-	V and R	
	Morphometrics	64	11.20	1.12	194.95	56.45	0.050		1
	Literature estimates	-	9.1-10		135-142.8		0.050-0.070		1.2
<i>Syracosphaera pulchra</i>	Birefringence	81	6.77	1.09	17.77	6.80	-	V, R and T	
	Morphometrics	81	6.77	1.09	26.94	11.16	0.030		1
	Literature estimates	-	2.7-6		13.5-16.5		0.027-0.083		1.2,4
<i>Umbellosphaera tenuis</i>	Birefringence	54	6.42	0.99	15.69	5.02	-	R	
	Morphometrics	54	6.42	0.99	11.45	4.61	0.015		1
	Literature estimates	-	5-6		8.7-23.9		0.015-0.071		1.2
<i>Umbilicosphaera sibogae</i>	Birefringence	6	7.76	1.81	27.14	11.07	-	V and R	
	Morphometrics	6	7.76	1.81	78.93	51.38	0.055		1
	Literature estimates	-	4.1-6		16-35		0.055-0.086		1.2

379 **Table 1:** Coccolith mass estimates of the main coccolithophore species found at the SOTS
 380 and SAM sites using birefringence (C-*Calcita*) and morphometrics. Additionally, length
 381 and mass estimates from the literature are also listed for most species. References: (1)
 382 Young and Ziveri (2000), (2) Beaufort and Heussner (1999), (3) Samtleben and Bickert
 383 (1990), (4) Poulton et al. (2010), (5) Poulton et al. (2011), (6) Holligan et al. (2010) and
 384 (7) Charalampopoulou et al. (2016). * coccolith mass range obtained applying the
 385 minimum and maximum k_s values for *E. huxleyi* found in the literature (i.e. 0.015 and
 386 0.04, respectively).



387

388 **Figure 4:** Average and standard deviation of the coccolith mass estimates of the most
 389 important coccolithophore species captured by the SOTS and SAM sediment traps using
 390 birefringence (C-*Calcita*) and morphometric approaches. For *E. huxleyi*, the
 391 morphometric-based coccolith mass estimate was calculated by applying a mean shape
 392 factor constant (k_s) value estimated from the range of all the morphotypes found at the
 393 SAZ (i.e. $k_s = 0.0275$, Table 1).



394

395 **Figure 5:** Inorganic carbon (CaCO₃) fluxes of coccolith calcite estimated using
 396 birefringence (C-*Calcita*) and morphometric approaches for the SOTS and SAM sites.

397 4. Discussion

398 4.1 Coccolithophore phenology in the SAZ: satellite versus sediment trap records

399 Total coccolith flux seasonality at the SOTS site shows good congruence with
 400 satellite-derived PIC in the surface layer, with both parameters suggesting enhanced



401 coccolithophore productivity between October and March (austral mid-spring to early
402 autumn; Fig. 2a). Interestingly, substantial coccosphere export ($> 1 \times 10^7$ coccospheres
403 $\text{m}^2 \text{d}^{-1}$) does not occur until January indicating that coccolith and coccosphere export are
404 not tightly coupled in the subantarctic waters south of Australia. Two different processes
405 could be invoked to explain the mismatch between coccolith and coccosphere fluxes at
406 this site. Firstly, *E. huxleyi*, the dominant coccolithophore species in the Southern Ocean,
407 is able to produce coccoliths rapidly (up to three coccoliths per hour; Paasche, 1962;
408 Balch et al., 1996) and shed the excess of coccoliths into the surrounding water under
409 certain environmental conditions (Paasche, 2002). Although the coccolith shedding rate
410 of *E. huxleyi* increases linearly with cellular growth rate (Fritz and Balch, 1996; Fritz,
411 1999), the tiny size and low weight of detached coccoliths allow them to remain in the
412 upper water column long after cell numbers have begun to decline. It follows that high
413 concentrations of detached coccoliths do not necessary imply a proportional abundance
414 of coccospheres in the surface layer (Tyrrell and Merico, 2004; Poulton et al., 2013) or in
415 the traps. Additionally, a substantial fraction of the coccospheres produced in the surface
416 layer may experience substantial mechanical breakage by zooplankton before reaching
417 the trap depths. Indeed, previous studies in the subantarctic waters south of Tasmania
418 demonstrated that microzooplankton grazing pressure is sufficient to remove up to 82%
419 of primary production in mid-summer (Pearce et al., 2011) and most of the particles
420 exported out the mixed layer during the productive period occur in the form of faecal
421 aggregates (Ebersbach et al., 2011). Therefore, it is highly likely that: (i) the intensity of
422 coccosphere export registered by the traps is influenced by grazing pressure in the surface
423 layer, and (ii) that the impact of grazing on coccolithophores varies throughout the year
424 (Calbet et al., 2008; Lawrence and Menden-Deuer, 2012; Quéguiner, 2013).

425 In contrast, seasonal variations in satellite-derived PIC concentration and
426 coccolith fluxes at SAM show some discrepancies not observed at SOTS. While
427 maximum PIC concentrations in the surface layer and coccolith and coccosphere fluxes
428 co-occur in December and January (austral early to mid-summer), satellite-derived PIC
429 suggests a secondary maximum in February-early-March not recorded by the trap (Fig.
430 2b). One possibility is that the satellite secondary maximum is not coccoliths. The higher
431 chlorophyll-a levels at the SAM site (Fig. 2) suggests that other phytoplankton groups,
432 such as diatoms, are more abundant than in the subantarctic waters south of Tasmania.
433 Empty and broken diatom valves have been suggested to display similar spectral
434 characteristics than those of coccolithophore blooms (Broerse et al., 2003; Tyrrell and



435 Merico, 2004; Winter et al., 2014). Therefore, the second peak in satellite-derived PIC
436 could have been caused by a senescent diatom bloom. This hypothesis is likely since
437 diatom blooms in the SAZ are known to develop early in the productive season (Rigual-
438 Hernández et al., 2015b) and rapidly decay following the depletion of silicate and/or iron
439 stocks in the surface layer (Lannuzel et al., 2011). However, no secondary late summer
440 maximum was observed in biogenic silica fluxes in the SAM. Another possible
441 explanation is a contribution to the satellite record from lithogenic material. Fully
442 resolving causes of mismatches between *in-situ* and satellite PIC estimates is not
443 achievable for the SAM site (nor more broadly for the Southern Ocean; Trull et al., 2018).

444 A second difference between the SAM and SOTS sites is that maximum annual
445 coccosphere export occurred one week earlier than maximum coccolith fluxes at SAM,
446 (Fig. 2). The different seasonalities between the sites suggest that different export
447 mechanisms may operate. The formation of rapidly sinking algal aggregates by diatoms
448 is known to scavenge particles they have collided with and increase particle sinking
449 (Alldredge and McGillivray, 1991; Passow and De La Rocha, 2006), thus the formation
450 of such rapid-sinking aggregates could potentially facilitate the preservation of
451 coccospheres early in the productive season at the SAM site. However, the lack of
452 accompanying *in situ* information on plankton community structure in the study region
453 precludes the assessment of these hypotheses.

454 Despite the uncertainties involved in our interpretations, the overall picture that
455 emerges from our comparison of satellite and sediment trap flux data is that the duration
456 of the coccolithophore bloom based on ocean-colour-based PIC concentrations most
457 likely provides an over-estimation of the coccolithophore productive season. Our
458 observations motivate caution in describing coccolithophore phenology solely based on
459 satellite-derived PIC concentrations (e.g. Hopkins et al., 2015).

460

461 **4.2 Magnitude and composition of subantarctic coccolithophore assemblages**

462 Annual coccolith export across the major zonal systems of the Australian sector
463 of the Southern Ocean exhibits a clear latitudinal gradient, with maximum fluxes at the
464 SAZ (8.6×10^{11} liths $m^{-2} yr^{-1}$) and eight-fold lower fluxes in the polar waters of the AZ
465 (1.0×10^{11} liths $m^{-2} yr^{-1}$; Rigual-Hernández et al., 2018). Coccolithophore species
466 occurrence documented by our subantarctic sediments traps are consistent with previous
467 reports on coccolithophore assemblage compositions in the surface layer (Findlay and



468 Giraudeau, 2000; Saavedra-Pellitero et al., 2014; Malinverno et al., 2015; Chang and
469 Northcote, 2016) and sediments (Findlay and Giraudeau, 2000; Saavedra-Pellitero and
470 Baumann, 2015) and are more diverse than those found in the AZ (Rigual Hernández et
471 al., 2018). The southward decline in coccolithophore abundance and diversity is most
472 likely due to the decrease in sea-surface temperature (SST) and light availability moving
473 poleward (Charalampopoulou et al., 2016; Trull et al., 2018). In particular, the close
474 relationship between temperature and growth rates has been demonstrated in a range of
475 coccolithophore species and strains (Buitenhuis et al., 2008), and seems to be a critical,
476 if not the most important, control on the biogeographical distribution of coccolithophore
477 species in the Southern Ocean (Trull et al., 2018). This pronounced latitudinal change in
478 coccolithophore assemblage composition contrasts with the little longitudinal variability
479 between the subantarctic SOTS and SAM sites (Fig. 3). These observations underscore
480 the role of circumpolar fronts as natural physical barriers for plankton species distribution
481 in the Southern Ocean (Medlin et al., 1994; Boyd, 2002; Cook et al., 2013).

482 Notably, the rare occurrence of the cold-water species *Coccolithus pelagicus* at
483 the SOTS and SAM sites contrasts with the high contribution of *C. pelagicus* to the living
484 coccolithophore communities in the subpolar and polar waters of the North Atlantic and
485 North Pacific oceans, where it is often the second most abundant species after *E. huxleyi*
486 (McIntyre and Bé, 1967; Baumann et al., 2000; Broerse et al., 2000a; Broerse et al.,
487 2000b; Ziveri et al., 2000). This important difference in species composition between
488 Northern and Southern hemisphere subpolar ecosystems could have important
489 implications in the calibration of the satellite PIC signal in the Southern Ocean. A recent
490 study by Trull et al. (2018) comparing satellite and shipboard observations identified a
491 substantial over-estimation of coccolithophore PIC in the Southern Ocean waters by the
492 NASA satellite ocean-colour-based PIC algorithm. Since satellite reflectance
493 observations are mainly calibrated against Northern Hemisphere PIC results (Balch et al.,
494 2011; Balch et al., 2016), we speculate that differences in the coccolithophore assemblage
495 composition, and particularly, differences in *C. pelagicus* numbers, could contribute to
496 the over-estimation of PIC concentrations by the satellite PIC algorithm in the Southern
497 Ocean. Indeed, the scaling of reflectance (in satellite images) to PIC (in ocean) is very
498 dependent on coccolith area:mass ratios (Gordon and Du, 2001; Balch et al., 2005).
499 *Coccolithus pelagicus* has remarkably heavier and thicker coccoliths (100-400 pg per
500 coccolith; Table 1) than *E. huxleyi* (~3 pg per coccolith), i.e. about 100 times heavier.
501 However, the average coccolith area of *C. pelagicus* is only about ten times greater than



502 that of *E. huxleyi*. Thus, this lack of proportional relationship between area and mass
503 between these species should be taken into consideration when calibrating the satellite
504 signals of coccolithophore-related PIC in the Southern Ocean.

505 **4.3 Coccolith calcite content of subantarctic coccolithophore species**

506 Multiple methodological biases associated with each of the methods used for
507 estimating coccolith calcite content (i.e. birefringence, morphometrics) could be invoked
508 to explain the different estimates observed for some of the species (see Young and Ziveri,
509 2000; Fuertes et al., 2014 and references therein). However, the fact that these
510 discrepancies vary greatly across species suggests that the composition of the crystal-
511 units of the coccoliths could be the most important factor causing these differences. All
512 the heterococcoliths of the species analysed are mainly composed of either V- or R-
513 calcite crystal units or a combination of both (Young et al., 2003; Table 1). R units are
514 characterized by sub-radial c-axes that are reasonably well measured by the birefringence
515 technique, but, the almost vertical optical axes of the V units (Young, 1992; Young et al.,
516 1999) make the same thickness less birefringent (Fuertes et al., 2014). Thus, it is likely
517 that differences in the birefringence properties of the R and V units could be responsible
518 for the different estimates provided by the two approaches. This is supported by our
519 results which show coccolith mass estimates of those species composed of R units, such
520 as *G. oceanica* and *Gephyrocapsa* spp. exhibit almost identical values with both
521 techniques (Table 1). In contrast, those species with coccoliths composed by a
522 combination of R and V units, such as *C. pelagicus*, *C. leptoporus*, *H. carteri* and *U.*
523 *sibogae*, display divergent mass estimates between approaches. The case of *E. huxleyi* is
524 more complex due to the large intraspecific genetic variability that results in substantial
525 differences in the profile and degree of calcification between specimens (Young and
526 Ziveri, 2000). Our birefringence mass estimate for *E. huxleyi* (2.67 ± 1.49 pg) is less than
527 one picogram lower than the mean range value calculated with the morphometric
528 technique (i.e. 1.81 ± 1.10 pg with an average k_s value of all the morphotypes found at
529 the SAZ, i.e. $k_s = 0.0275$), but identical to the maximum (2.64 ± 1.60 pg; using $k_s = 0.04$).
530 These results suggest a reasonably good consistency between techniques for *E. huxleyi*.

531 Taking into consideration all the above, it is likely that the coccolith mass of some
532 species is underestimated by the birefringence technique, and therefore, the fractional
533 contribution of coccolithophores to total PIC using this approach should be taken as a
534 conservative estimate. Since both methods for estimating calcite content have inherent



535 uncertainties, the range of values provided by both techniques is used here as an
536 approximation of the fractional contribution of coccolithophores to total annual CaCO_3
537 export to the deep sea in the Australian and New Zealand sectors of the SAZ.

538 **4.4 Contribution of coccolithophores to carbonate export in the Australian-New** 539 **Zealand sectors of the Southern Ocean**

540 The magnitude of the total PIC export in the subantarctic waters was similar
541 between the SOTS and SAM sites (range $14\text{-}17\text{ g m}^{-2}\text{ yr}^{-1}$), and thus slightly above the
542 global average ($11\text{ g m}^{-2}\text{ yr}^{-1}$; Honjo et al., 2008). Our estimates indicate that
543 coccolithophores are major contributors to CaCO_3 export in the Australian and New
544 Zealand waters of the SAZ, accounting for 40-60% and 15-25% of the annual CaCO_3
545 export, respectively (Fig. 5). Heterotrophic calcifiers, mainly planktonic foraminifera
546 (Salter et al., 2014), must therefore account for the remainder of the annual CaCO_3 export
547 at both sites. Previous work on foraminifera fluxes in our study regions allows an
548 approximate estimate of the contribution of foraminifera to total CaCO_3 flux that can be
549 used to assess the validity of our estimates. Combining counts of foraminifera
550 shells (King and Howard, 2003) with estimates of their average shell weights ($20\text{-}40\text{ }\mu\text{g}$
551 per shell depending on size; Moy et al., 2009) suggests contributions of 1/3 to 2/3 of
552 planktonic foraminifera to the total CaCO_3 flux in the Australian SAZ (Trull et al., 2018).
553 In the subantarctic waters south of New Zealand, Northcote and Neil (2005) estimated
554 that planktonic foraminifera accounted for about 78-97% of the total CaCO_3 . Thus
555 estimations of the contribution of heterotrophic calcifiers to total carbonate in both study
556 regions are in reasonable agreement with our coccolithophore CaCO_3 estimates at both
557 sites. The lower contribution of coccolithophores to CaCO_3 export at the SAM site in
558 comparison with that of SOTS may be explained by differences in the ecosystem structure
559 between sites. Algal biomass accumulation in the surface waters of the SAM region
560 (average chlorophyll-*a* concentration between 2002 and 2018 is 0.31 mg m^{-3}) is
561 substantially higher than that at SOTS (0.23 mg m^{-3}). We speculate that the higher
562 abundance of non-calcareous phytoplankton (e.g. diatoms) in the subantarctic waters
563 south of New Zealand could simultaneously reduce coccolithophore biomass through
564 resource competition (Quééré et al., 2005; Sinha et al., 2010) while stimulating
565 foraminifera growth (Schiebel et al., 2017). The combination of both factors could be
566 responsible for the lower coccolithophore productivity at the SAM site despite similar
567 total CaCO_3 export. Assuming that both the SOTS and SAM sites can be considered



568 representative of a broad longitudinal swath of the SAZ south of Australia and New
569 Zealand (ca. 1% of areal extent of the global ocean), the coccolithophore CaCO_3 export
570 in these two regions together account for approximately $0.4 \text{ T C}_{\text{inorg}} \text{ mol yr}^{-1}$. This value
571 represents approximately 1% of the global annual PIC export to the deep ocean (Honjo et
572 al., 2008) and underscores the notion that the high nutrient low-chlorophyll waters of the
573 circumpolar SAZ should not be taken as indicative of low biological activity or export.

574 Our results indicate that although *E. huxleyi* overwhelmingly dominates the
575 coccolithophore sinking assemblages at both study sites, other species with lower relative
576 contribution but substantially heavier coccoliths are more important contributors to the
577 annual coccolithophore CaCO_3 export budget (Fig. 3). Particularly relevant is the case of
578 *C. leptoporus* that despite its relatively low abundance (~ 10% of the annual assemblage
579 at both sites; Fig. 3), it accounts for between 30-50% and 60-70% of the annual
580 coccolithophore- CaCO_3 export at the SOTS and SAM sites, respectively (Fig. 3).
581 Similarly, other species with heavy coccoliths, such as *H. carteri* and *C. pelagicus*, are
582 important contributors to the annual coccolithophore PIC export to the deep sea (up to
583 ~30% and ~10% of the annual coccolithophore PIC, respectively) despite their low annual
584 relative abundance (<2% at both sites) (Fig. 3). These results serve as an important
585 reminder that it is often not the most abundant species, but rather the largest
586 coccolithophore species that account for the greatest contribution to coccolithophore
587 CaCO_3 production and export (Young and Ziveri, 2000; Baumann et al., 2004; Daniels et
588 al., 2016).

589 The important contribution made by the coccolithophore community in setting the
590 magnitude of carbonate production and export to the deep sea is evidenced when we
591 compare the coccolith and total CaCO_3 fluxes of the SOTS sediment trap with those
592 deployed in the AZ along the 140°E meridian (Fig. 1). Although both total and
593 coccolithophore CaCO_3 export decrease with increasing latitude these changes are largely
594 uneven. While total CaCO_3 decreases two-fold from the SAZ to the AZ, coccolithophore
595 CaCO_3 export decreases 28-fold (Supplement Figure 2). This lack of proportional
596 latitudinal change can be attributed to two main factors. First, subantarctic
597 coccolithophore populations are diverse and relatively rich in species with large and
598 heavy coccoliths such as *C. leptoporus* or *H. carteri* that account for a large fraction of
599 the annual carbonate production and export. South of the PF, assemblages become
600 monospecific, or nearly monospecific, dominated by the small and relatively lightly



601 calcified *E. huxleyi*. Second, latitudinal variations in the abundance of heterotrophic
602 calcifiers (mainly foraminifera but also pteropods) must play a major role in modulating
603 the observed variations in CaCO₃ export. In particular, our data suggests that the
604 fractional contribution of heterotrophic calcifiers to CaCO₃ production increases from
605 ~40-60 % in the Australian SAZ to up to 95% in the AZ (Rigual Hernández et al., 2018).
606 This pattern is consistent with previous shipboard and sediment trap studies that reported
607 higher abundances of planktonic foraminifera at the PFZ and AZ compared to that of the
608 SAZ in the Australian sector (King and Howard, 2003; Trull et al., 2018). Controls on the
609 biogeographic distribution of foraminifera species are complex and beyond the scope of
610 this paper, however, we provide a few observations. Both temperature and diet are critical
611 factors controlling the spatial distribution of planktonic foraminifera species. In
612 particular, the lower temperatures south of the SAF seem to favour the development of
613 *Neogloboquadrina pachyderma* sin. and *Turborotalita quinqueloba* as indicated by the
614 high abundance of these species in the PFZ (> 80% of the annual integrated flux for both
615 species together; King and Howard, 2003). Additionally, the dramatically different algal
616 communities dwelling in each zonal system may also play a role in planktonic
617 foraminifera species distributions. In particular, diatoms can account for a major part of
618 the diet of some foraminifera species, including *N. pachyderma* (Schiebel and Hemleben,
619 2017). Therefore, it is likely that the preferential grazing on diatoms of some foraminifera
620 species may play an important role in the increase of foraminifera CaCO₃ production
621 moving poleward.

622

623 **4.5 Future predictions of coccolithophore community response to environmental** 624 **change in the subantarctic zone**

625 The response of *E. huxleyi* to environmental change has been extensively studied
626 in laboratory experiments (Meyer and Riebesell, 2015; Müller et al., 2015; Feng et al.,
627 2017) and the available information is sufficient to propose possible changes of its niche
628 and calcification in the Southern Ocean, as discussed in detail in Trull et al. (2018). Due
629 to the ubiquity and abundance of *E. huxleyi*, the ecophysiology of this species is often
630 regarded as typical of all coccolithophores. However, *E. huxleyi* is rather different from
631 most other coccolithophore species in that its physiological adaptations place it in the
632 upper limit of the r-K ecological gradient of these organisms (i.e. an opportunistic
633 species), while most of the other species are located at the opposite end of the spectrum



634 (i.e. conservative or K-selected species) (Probert and Houdan, 2004). Our results
635 demonstrate that *E. huxleyi* plays an important, but not dominant role in CaCO₃ export,
636 with other species such as *C. leptoporus*, *H. carteri* or *C. pelagicus* making a larger
637 contribution to the annual CaCO₃ export in the SAZ (Fig. 3). Therefore, it is of critical
638 importance to evaluate how these other biogeochemically important coccolithophore
639 species will respond to projected climate-induced changes in the Southern Ocean. Here,
640 we now assess the response of large coccolithophore species to projected changes in
641 temperature and carbonate chemistry, that have been highlighted among the most
642 important environmental stressors expected to impact Southern Ocean coccolithophore
643 physiological rates (Müller et al., 2015; Charalampopoulou et al., 2016; Feng et al., 2017;
644 Trull et al., 2018).

645 The Southern Ocean is warming rapidly (Gille, 2002; Böning et al., 2008), largely
646 due to the southward migration of the ACC fronts (Sokolov and Rintoul, 2009). Only
647 between 1992 and 2007 the position of Southern Ocean fronts shifted by approximately
648 60 km to the south (Sokolov and Rintoul, 2009) and this trend is expected to continue
649 throughout the next century (Rintoul et al., 2018). Therefore, it is likely that any further
650 southward migration of ACC fronts will be coupled with an expansion of subantarctic
651 coccolithophore species towards higher latitudes. The poleward expansion of *E. huxleyi*
652 geographic range has already been suggested in the Southern Ocean (Cubillos et al., 2007;
653 Winter et al., 2014; Charalampopoulou et al., 2016) and it also appears to be occurring in
654 the North Atlantic (Rivero-Calle et al., 2015). Given the important contribution of large
655 subantarctic coccolithophore species to CaCO₃ export, the expansion of their ecological
656 niche could result in a substantial increase in CaCO₃ production and export in the
657 Southern Ocean. However, this may not be the future scenario for the SAZ southeast on
658 New Zealand, where bathymetry strongly controls the location of ocean fronts (Fernandez
659 et al., 2014; Chiswell et al., 2015). If the fronts are bathymetrically ‘locked’, then the
660 SAZ will not expand in areal extent, although the region is still predicted to undergo
661 significant physical, biogeochemical and biological changes (Law et al., 2017) that will
662 have likely flow-on effects on coccolithophore productivity and export (Deppeler and
663 Davidson, 2017).

664 The available carbonate chemistry manipulation experiments with *C. leptoporus*
665 have come to different conclusions. While some studies identified an increase in coccolith
666 malformations with increasing CO₂ concentrations (Langer et al., 2006; Langer and Bode,
667 2011; Diner et al., 2015), another study (Fiorini et al., 2011) reported no changes in the



668 calcification of *C. leptoporus* at elevated $p\text{CO}_2$. Interestingly, *C. leptoporus* did not
669 experience changes in its photosynthesis rates over the tested CO_2 range in any of the
670 aforementioned studies. The most likely explanation for the different results between the
671 studies is a strain-specific variable responses to changing carbonate chemistry (Diner et
672 al., 2015). Strain-specific variability in response to changing carbonate chemistry has
673 been previously reported in other coccolithophores, such as *E. huxleyi* (Langer et al.,
674 2009; Müller et al., 2015), and therefore it is likely that this also occurs in other species.
675 Given the fact that Southern Ocean fronts act as barriers for species distributions and gene
676 flows (Medlin et al., 1994; Patarnello et al., 1996; Thornhill et al., 2008; Cook et al.,
677 2013), it is possible that the subantarctic *C. leptoporus* populations exhibit a different
678 ecophysiology than those used in the above mentioned laboratory experiments. Prediction
679 of the responses of *H. carteri* and *C. pelagicus* is even more challenging due to the lack
680 of experiments testing the response of these species to changing seawater carbonate
681 chemistry. The only available insights in the response of one of these species to ocean
682 acidification are found in the fossil record. Both Gibbs et al. (2013) and O’Dea et al.
683 (2014) reconstructed the evolution of *C. pelagicus* populations during the Palaeocene-
684 Eocene Thermal Maximum (PETM), a period arguably regarded as the best geological
685 approximation of the present rapid rise in atmospheric CO_2 levels and temperatures.
686 These studies concluded that *C. pelagicus* most likely reduced its growth rates and
687 calcification during this period. This limited number of studies suggest that the ongoing
688 ocean acidification in the Southern Ocean could potentially have a negative impact on the
689 physiological rates of *C. leptoporus* and *C. pelagicus* while the effect on *H. carteri* is
690 unknown. Physiological response experiments (e.g. Müller et al., 2015) with Southern
691 Ocean strains of *C. leptoporus*, *H. carteri* and *C. pelagicus* are, therefore, urgently needed
692 to be able to quantify the effect of projected changes in oceanic conditions in the SAZ on
693 their physiological rates and consequent effects on carbon cycling in the Southern Ocean.

694 Our synthesis suggests opposing influence of environmental stressors on
695 subantarctic coccolithophore populations. Poleward migration of fronts will likely
696 increase coccolithophore CaCO_3 production in the Southern Ocean, while changes in
697 carbonate chemistry speciation will reduce growth rates of subantarctic coccolithophores.
698 It seems possible that coccolithophores will initially expand southward as waters warm
699 and fronts migrate, but then eventually diminish as acidification overwhelms those
700 changes.



701

702 **Acknowledgments**

703 This project has received funding from the European Union's Horizon 2020 research and
704 innovation programme under the Marie Skłodowska-Curie grant agreement number
705 748690 – SONAR-CO2 (ARH, JAF and FA). The SOTS mooring work was supported
706 by IMOS, the ACE CRC, and the Australian Marine National Facility. The work at SAM
707 was supported by funding provided by the New Zealand Ministry of Business, Innovation
708 and Employment and previous agencies, and most recently by NIWA's Strategic Science
709 Investment Fund. NIWA is acknowledged for providing capital grants for mooring
710 equipment purchases, and thanks to all the NIWA scientists, technicians and vessels staff,
711 who participated in the New Zealand biophysical moorings programme (2000-12).
712 Cathryn Wynn-Edwards (IMAS) provided support in sample splitting/processing and
713 laboratory analysis. Satellite Chlorophyll-*a* and PIC data sets were produced with the
714 Giovanni online data system, developed
715 and maintained by the NASA GES DISC.

716

717 **Author contributions**

718 TWT, SDN, DMD and LN planned and performed the field experiment. ARH led the
719 coccolithophore study and performed sample processing and microscopy and image
720 analyses. AMB and ARH performed SEM analyses. ARH and SN performed numerical
721 analyses. ARH wrote the paper with feedback from all authors.



722 **Competing interests**

723 The authors declare no competing interests.

724

725 **Data Availability**

726 Morphometric data of major coccolithophore species generated during the current study are listed
727 in Table 1, while species relative abundance and species fluxes (plotted in Supplement Figure 1)
728 will be publicly available through the Australian Antarctic Data Centre (link to be included before
729 publication).

730

731 **References**

732 Alldredge, A. L., and McGillivray, P.: The attachment probabilities of marine snow and
733 their implications for particle coagulation in the ocean, *Deep Sea Research Part A*.
734 *Oceanographic Research Papers*, 38, 431-443, [http://dx.doi.org/10.1016/0198-](http://dx.doi.org/10.1016/0198-0149(91)90045-H)
735 [0149\(91\)90045-H](http://dx.doi.org/10.1016/0198-0149(91)90045-H), 1991.

736 Alvain, S., Le Quéré, C., Bopp, L., Racault, M.-F., Beaugrand, G., Dessailly, D., and
737 Buitenhuis, E. T.: Rapid climatic driven shifts of diatoms at high latitudes, *Remote*
738 *Sensing of Environment*, 132, 195-201, <http://dx.doi.org/10.1016/j.rse.2013.01.014>,
739 2013.

740 Bairbakhish, A. N., Bollmann, J., Sprengel, C., and Thierstein, H. R.: Disintegration of
741 aggregates and coccospheres in sediment trap samples, *Marine Micropaleontology*, 37,
742 219-223, [http://dx.doi.org/10.1016/S0377-8398\(99\)00019-5](http://dx.doi.org/10.1016/S0377-8398(99)00019-5), 1999.

743 Balch, W. M., Fritz, J., and Fernandez, E.: Decoupling of calcification and
744 photosynthesis in the coccolithophore *Emiliania huxleyi* under steady-state light-limited
745 growth, *Marine Ecology Progress Series*, 142, 87-97, 1996.

746 Balch, W. M., Gordon, H. R., Bowler, B. C., Drapeau, D. T., and Booth, E. S.: Calcium
747 carbonate measurements in the surface global ocean based on Moderate-Resolution
748 Imaging Spectroradiometer data, 110, doi:10.1029/2004JC002560, 2005.

749 Balch, W. M., Drapeau, D. T., Bowler, B. C., Lyczkowski, E., Booth, E. S., and Alley,
750 D.: The contribution of coccolithophores to the optical and inorganic carbon budgets
751 during the Southern Ocean Gas Exchange Experiment: New evidence in support of the
752 “Great Calcite Belt” hypothesis, *Journal of Geophysical Research: Oceans*, 116, n/a-n/a,
753 10.1029/2011JC006941, 2011.

754 Balch, W. M., Bates, N. R., Lam, P. J., Twining, B. S., Rosengard, S. Z., Bowler, B. C.,
755 Drapeau, D. T., Garley, R., Lubelczyk, L. C., Mitchell, C., and Rauschenberg, S.:
756 Factors regulating the Great Calcite Belt in the Southern Ocean and its biogeochemical



757 significance, *Global Biogeochemical Cycles*, 30, 1124-1144, 10.1002/2016GB005414,
758 2016.

759 Baumann, K.-H., Böckel, B., and Frenz, M.: Coccolith contribution to South Atlantic
760 carbonate sedimentation, in: *Coccolithophores: From Molecular Processes to Global*
761 *Impact*, edited by: Thierstein, H. R., and Young, J. R., Springer Berlin Heidelberg,
762 Berlin, Heidelberg, 367-402, 2004.

763 Baumann, K. H., Andruleit, H., and Samtleben, C.: Coccolithophores in the Nordic
764 Seas: comparison of living communities with surface sediment assemblages, *Deep Sea*
765 *Research Part II: Topical Studies in Oceanography*, 47, 1743-1772,
766 [http://dx.doi.org/10.1016/S0967-0645\(00\)00005-9](http://dx.doi.org/10.1016/S0967-0645(00)00005-9), 2000.

767 Beaufort, L., and Heussner, S.: Coccolithophorids on the continental slope of the Bay of
768 Biscay – production, transport and contribution to mass fluxes, *Deep Sea Research Part*
769 *II: Topical Studies in Oceanography*, 46, 2147-2174, [https://doi.org/10.1016/S0967-](https://doi.org/10.1016/S0967-0645(99)00058-2)
770 [0645\(99\)00058-2](https://doi.org/10.1016/S0967-0645(99)00058-2), 1999.

771 Beaufort, L.: Weight estimates of coccoliths using the optical properties (birefringence)
772 of calcite, *Micropaleontology*, 51, 289-297, 10.2113/gsmicropal.51.4.289, 2005.

773 Beaufort, L., Barbarin, N., and Gally, Y.: Optical measurements to determine the
774 thickness of calcite crystals and the mass of thin carbonate particles such as coccoliths,
775 *Nature Protocols*, 9, 633, 10.1038/nprot.2014.028
776 <https://www.nature.com/articles/nprot.2014.028#supplementary-information>, 2014.

777 Bolton, C. T., Hernandez-Sanchez, M. T., Fuertes, M.-A., Gonzalez-Lemos, S.,
778 Abrevaya, L., Mendez-Vicente, A., Flores, J.-A., Probert, I., Giosan, L., Johnson, J., and
779 Stoll, H. M.: Decrease in coccolithophore calcification and CO₂ since the middle
780 Miocene, *Nat Commun*, 7, 10.1038/ncomms10284, 2016.

781 Böning, C. W., Dispert, A., Visbeck, M., Rintoul, S. R., and Schwarzkopf, F. U.: The
782 response of the Antarctic Circumpolar Current to recent climate change, *Nature*
783 *Geoscience*, 1, 864, 10.1038/ngeo362
784 <https://www.nature.com/articles/ngeo362#supplementary-information>, 2008.

785 Bowie, A. R., Brian Griffiths, F., Dehairs, F., and Trull, T.: Oceanography of the
786 subantarctic and Polar Frontal Zones south of Australia during summer: Setting for the
787 SAZ-Sense study, *Deep Sea Research Part II: Topical Studies in Oceanography*, 58,
788 2059-2070, <http://dx.doi.org/10.1016/j.dsr2.2011.05.033>, 2011.



- 789 Boyd, P. W.: Environmental factors controlling phytoplankton processes in the
790 Southern Ocean, *Journal of Phycology*, 38, 844-861, 10.1046/j.1529-8817.2002.t01-1-
791 01203.x, 2002.
- 792 Boyd, P. W., and Trull, T. W.: Understanding the export of biogenic particles in oceanic
793 waters: Is there consensus?, *Progress in Oceanography*, 72, 276-312,
794 <http://dx.doi.org/10.1016/j.pocean.2006.10.007>, 2007.
- 795 Broerse, A. T. C., Ziveri, P., and Honjo, S.: Coccolithophore (–CaCO₃) flux in the Sea
796 of Okhotsk: seasonality, settling and alteration processes, *Marine Micropaleontology*,
797 39, 179-200, [https://doi.org/10.1016/S0377-8398\(00\)00020-7](https://doi.org/10.1016/S0377-8398(00)00020-7), 2000a.
- 798 Broerse, A. T. C., Ziveri, P., van Hinte, J. E., and Honjo, S.: Coccolithophore export
799 production, species composition, and coccolith–CaCO₃ fluxes in the NE Atlantic
800 (34°N21°W and 48°N21°W), *Deep Sea Research Part II: Topical Studies in*
801 *Oceanography*, 47, 1877-1905, [https://doi.org/10.1016/S0967-0645\(00\)00010-2](https://doi.org/10.1016/S0967-0645(00)00010-2), 2000b.
- 802 Broerse, A. T. C., Tyrrell, T., Young, J. R., Poulton, A. J., Merico, A., Balch, W. M.,
803 and Miller, P. I.: The cause of bright waters in the Bering Sea in winter, *Continental*
804 *Shelf Research*, 23, 1579-1596, <https://doi.org/10.1016/j.csr.2003.07.001>, 2003.
- 805 Buitenhuis, E. T., Wal, P., and Baar, H. J. W.: Blooms of *Emiliana huxleyi* are sinks of
806 atmospheric carbon dioxide: A field and mesocosm study derived simulation, *Global*
807 *Biogeochemical Cycles*, 15, 577-587, doi:10.1029/2000GB001292, 2001.
- 808 Buitenhuis, E. T., Pangerc, T., Franklin, D. J., Le Quéré, C., and Malin, G.: Growth
809 rates of six coccolithophorid strains as a function of temperature, 53, 1181-1185,
810 doi:10.4319/lo.2008.53.3.1181, 2008.
- 811 Calbet, A., Trepát, I., Almeda, R., Salá, V., Saiz, E., Movilla, J. I., Alcaraz, M.,
812 Yebra, L., and Simó, R.: Impact of micro- and nanograzers on phytoplankton
813 assessed by standard and size-fractionated dilution grazing experiments, *Aquatic*
814 *Microbial Ecology*, 50, 145-156, 2008.
- 815 Cao, L., and Caldeira, K.: Atmospheric CO₂ stabilization and ocean acidification,
816 *Geophysical Research Letters*, 35, n/a-n/a, 10.1029/2008GL035072, 2008.
- 817 Chang, F. H., and Gall, M.: Phytoplankton assemblages and photosynthetic pigments
818 during winter and spring in the Subtropical Convergence region near New Zealand,
819 *New Zealand Journal of Marine and Freshwater Research*, 32, 515-530,
820 10.1080/00288330.1998.9516840, 1998.



- 821 Chang, F. H., and Northcote, L.: Species composition of extant coccolithophores
822 including twenty six new records from the southwest Pacific near New Zealand, *Marine*
823 *Biodiversity Records*, 9, 75, 10.1186/s41200-016-0077-7, 2016.
- 824 Charalampopoulou, A., Poulton, A. J., Bakker, D. C., Lucas, M. I., Stinchcombe, M. C.,
825 and Tyrrell, T. J. B.: Environmental drivers of coccolithophore abundance and
826 calcification across Drake Passage (Southern Ocean), 13, 5917-5935, 2016.
- 827 Chiswell, S. M., Bostock, H. C., Sutton, P. J. H., and Williams, M. J. M.: Physical
828 oceanography of the deep seas around New Zealand: a review, *New Zealand Journal of*
829 *Marine and Freshwater Research*, 49, 286-317, 10.1080/00288330.2014.992918, 2015.
- 830 Cook, S. S., Jones, R. C., Vaillancourt, R. E., and Hallegraeff, G. M.: Genetic
831 differentiation among Australian and Southern Ocean populations of the ubiquitous
832 coccolithophore *Emiliania huxleyi* (Haptophyta), *Phycologia*, 52, 368-374, 10.2216/12-
833 111.1, 2013.
- 834 Cubillos, J., Wright, S., Nash, G., De Salas, M., Griffiths, B., Tilbrook, B., Poisson, A.,
835 and Hallegraeff, G.: Calcification morphotypes of the coccolithophorid *Emiliania*
836 *huxleyi* in the Southern Ocean: changes in 2001 to 2006 compared to historical data,
837 *Marine Ecology Progress Series*, 348, 47-54, 2007.
- 838 D’Amario, B., Ziveri, P., Grelaud, M., and Oviedo, A.: *Emiliania huxleyi* coccolith
839 calcite mass modulation by morphological changes and ecology in the Mediterranean
840 Sea, *PLOS ONE*, 13, e0201161, 10.1371/journal.pone.0201161, 2018.
- 841 Daniels, C. J., Poulton, A. J., Young, J. R., Esposito, M., Humphreys, M. P., Ribas-
842 Ribas, M., Tynan, E., and Tyrrell, T.: Species-specific calcite production reveals
843 *Coccolithus pelagicus* as the key calcifier in the Arctic Ocean, *Marine Ecology Progress*
844 *Series*, 555, 29-47, 2016.
- 845 de Salas, M. F., Eriksen, R., Davidson, A. T., and Wright, S. W.: Protistan communities
846 in the Australian sector of the Sub-Antarctic Zone during SAZ-Sense, *Deep Sea*
847 *Research Part II: Topical Studies in Oceanography*, 58, 2135-2149,
848 <http://dx.doi.org/10.1016/j.dsr2.2011.05.032>, 2011.
- 849 Deppeler, S. L., and Davidson, A. T.: Southern Ocean Phytoplankton in a Changing
850 Climate, *Frontiers in Marine Science*, 4, 10.3389/fmars.2017.00040, 2017.
- 851 Diner, R. E., Benner, I., Passow, U., Komada, T., Carpenter, E. J., and Stillman, J. H. J.
852 M. B.: Negative effects of ocean acidification on calcification vary within the
853 coccolithophore genus *Calcidiscus*, 162, 1287-1305, 10.1007/s00227-015-2669-x, 2015.



- 854 Dugdale, R. C., Wilkerson, F. P., and Minas, H. J.: The role of a silicate pump in
855 driving new production, *Deep Sea Research Part I: Oceanographic Research Papers*, 42,
856 697-719, [http://dx.doi.org/10.1016/0967-0637\(95\)00015-X](http://dx.doi.org/10.1016/0967-0637(95)00015-X), 1995.
- 857 Ebersbach, F., Trull, T. W., Davies, D. M., and Bray, S. G.: Controls on mesopelagic
858 particle fluxes in the Sub-Antarctic and Polar Frontal Zones in the Southern Ocean
859 south of Australia in summer—Perspectives from free-drifting sediment traps, *Deep Sea*
860 *Research Part II: Topical Studies in Oceanography*, 58, 2260-2276,
861 <http://dx.doi.org/10.1016/j.dsr2.2011.05.025>, 2011.
- 862 Eriksen, R., Trull, T. W., Davies, D., Jansen, P., Davidson, A. T., Westwood, K., and
863 van den Enden, R.: Seasonal succession of phytoplankton community structure from
864 autonomous sampling at the Australian Southern Ocean Time Series (SOTS)
865 observatory, *Marine Ecology Progress Series*, 589, 13-31, 2018.
- 866 Fabry, V. J., McClintock, J. B., Mathis, J. T., and Grebmeier, J. M.: Ocean acidification
867 at high latitudes: the bellweather, *Oceanography*, 22, 160, 2009.
- 868 Feng, Y., Roleda, M. Y., Armstrong, E., Boyd, P. W., and Hurd, C. L.: Environmental
869 controls on the growth, photosynthetic and calcification rates of a Southern Hemisphere
870 strain of the coccolithophore *Emiliana huxleyi*, *Limnology and Oceanography*, 62, 519-
871 540, 10.1002/lno.10442, 2017.
- 872 Fernandez, D., Bowen, M., and Carter, L.: Intensification and variability of the
873 confluence of subtropical and subantarctic boundary currents east of New Zealand,
874 *Journal of Geophysical Research: Oceans*, 119, 1146-1160, 10.1002/2013jc009153,
875 2014.
- 876 Findlay, C. S., and Giraudeau, J.: Extant calcareous nannoplankton in the Australian
877 Sector of the Southern Ocean (austral summers 1994 and 1995), *Marine*
878 *Micropaleontology*, 40, 417-439, [http://dx.doi.org/10.1016/S0377-8398\(00\)00046-3](http://dx.doi.org/10.1016/S0377-8398(00)00046-3),
879 2000.
- 880 Fiorini, S., Middelburg, J. J., and Gattuso, J.-P.: Testing the effects of elevated pCO₂ on
881 coccolithophores (Prymnesiophyceae): comparison between haploid and diploid life
882 stages, 47, 1281-1291, doi:10.1111/j.1529-8817.2011.01080.x, 2011.
- 883 Flores, J. A., and Sierro, F. J.: A revised technique for the calculation of calcareous
884 nannofossil accumulation rates., *Micropaleontology*, 43, 321-324, 1997.
- 885 Fritz, J. J., and Balch, W. M.: A light-limited continuous culture study of *Emiliana*
886 *huxleyi*: determination of coccolith detachment and its relevance to cell sinking, *Journal*



887 of Experimental Marine Biology and Ecology, 207, 127-147,
888 [https://doi.org/10.1016/S0022-0981\(96\)02633-0](https://doi.org/10.1016/S0022-0981(96)02633-0), 1996.
889 Fritz, J. J.: Carbon fixation and coccolith detachment in the coccolithophore *Emiliana*
890 *huxleyi* in nitrate-limited cyclostats, *Marine Biology*, 133, 509-518,
891 10.1007/s002270050491, 1999.
892 Fuertes, M.-Á., Flores, J.-A., and Sierro, F. J.: The use of circularly polarized light for
893 biometry, identification and estimation of mass of coccoliths, *Marine*
894 *Micropaleontology*, 113, 44-55, <http://dx.doi.org/10.1016/j.marmicro.2014.08.007>,
895 2014.
896 Gattuso, J.-P., and Hansson, L.: *Ocean acidification*, Oxford University Press, 2011.
897 Gibbs, S. J., Poulton, A. J., Bown, P. R., Daniels, C. J., Hopkins, J., Young, J. R., Jones,
898 H. L., Thiemann, G. J., O’Dea, S. A., and Newsam, C.: Species-specific growth
899 response of coccolithophores to Palaeocene–Eocene environmental change, *Nature*
900 *Geoscience*, 6, 218, 10.1038/ngeo1719
901 <https://www.nature.com/articles/ngeo1719#supplementary-information>, 2013.
902 Gille, S. T.: Warming of the Southern Ocean Since the 1950s, *Science*, 295, 1275-1277,
903 10.1126/science.1065863, 2002.
904 González Lemos, S., Guitián, J., Fuertes, M.-Á., Flores, J.-A., and Stoll, H. M.: An
905 empirical method for absolute calibration of coccolith thickness, *Biogeosciences*, 15,
906 2018.
907 Gordon, H. R., and Du, T.: Light scattering by nonspherical particles: Application to
908 coccoliths detached from *Emiliana huxleyi*, *Limnology and Oceanography*, 46, 1438-
909 1454, 10.4319/lo.2001.46.6.1438, 2001.
910 Gravalosa, J. M., Flores, J.-A., Sierro, F. J., and Gersonde, R.: Sea surface distribution
911 of coccolithophores in the eastern Pacific sector of the Southern Ocean (Bellingshausen
912 and Amundsen Seas) during the late austral summer of 2001, *Marine*
913 *Micropaleontology*, 69, 16-25, <https://doi.org/10.1016/j.marmicro.2007.11.006>, 2008.
914 Herraiz-Borreguero, L., and Rintoul, S. R.: Regional circulation and its impact on upper
915 ocean variability south of Tasmania, *Deep Sea Research Part II: Topical Studies in*
916 *Oceanography*, 58, 2071-2081, <http://dx.doi.org/10.1016/j.dsr2.2011.05.022>, 2011.
917 Holligan, P. M., Charalampopoulou, A., and Hutson, R.: Seasonal distributions of the
918 coccolithophore, *Emiliana huxleyi*, and of particulate inorganic carbon in surface



- 919 waters of the Scotia Sea, *Journal of Marine Systems*, 82, 195-205,
920 <http://dx.doi.org/10.1016/j.jmarsys.2010.05.007>, 2010.
- 921 Honjo, S., Manganini, S. J., Krishfield, R. A., and Francois, R.: Particulate organic
922 carbon fluxes to the ocean interior and factors controlling the biological pump: A
923 synthesis of global sediment trap programs since 1983, *Progress in Oceanography*, 76,
924 217-285, <http://dx.doi.org/10.1016/j.pocean.2007.11.003>, 2008.
- 925 Hopkins, J., Henson, S. A., Painter, S. C., Tyrrell, T., and Poulton, A. J.: Phenological
926 characteristics of global coccolithophore blooms, *Global Biogeochemical Cycles*, 29,
927 239-253, 10.1002/2014GB004919, 2015.
- 928 King, A. L., and Howard, W. R.: Planktonic foraminiferal flux seasonality in
929 Subantarctic sediment traps: A test for paleoclimate reconstructions, *Paleoceanography*,
930 18, 1019, 10.1029/2002pa000839, 2003.
- 931 Kocczynska, E. E., Dehairs, F., Elskens, M., and Wright, S.: Phytoplankton and
932 microzooplankton variability between the Subtropical and Polar Fronts south of
933 Australia: Thriving under regenerative and new production in late summer, *Journal of*
934 *Geophysical Research: Oceans*, 106, 31597-31609, 10.1029/2000JC000278, 2001.
- 935 Langer, G., Geisen, M., Baumann, K.-H., Kläs, J., Riebesell, U., Thoms, S., and Young,
936 J. R.: Species-specific responses of calcifying algae to changing seawater carbonate
937 chemistry, *Geochemistry, Geophysics, Geosystems*, 7, n/a-n/a,
938 10.1029/2005GC001227, 2006.
- 939 Langer, G., Nehrke, G., Probert, I., Ly, J., and Ziveri, P.: Strain-specific responses of
940 *Emiliania huxleyi* to changing seawater carbonate chemistry, *Biogeosciences*, 6, 2637-
941 2646, 2009.
- 942 Langer, G., and Bode, M. J. G., *Geophysics, Geosystems: CO₂ mediation of adverse*
943 *effects of seawater acidification in Calcidiscus leptoporus*, 12, 2011.
- 944 Lannuzel, D., Bowie, A. R., Remenyi, T., Lam, P., Townsend, A., Ibanmi, E., Butler,
945 E., Wagener, T., and Schoemann, V.: Distributions of dissolved and particulate iron in
946 the sub-Antarctic and Polar Frontal Southern Ocean (Australian sector), *Deep Sea*
947 *Research Part II: Topical Studies in Oceanography*, 58, 2094-2112,
948 <http://dx.doi.org/10.1016/j.dsr2.2011.05.027>, 2011.
- 949 Law, C. S., Schwarz, J. N., Chang, F. H., Nodder, S. D., Northcote, L. C., Safi, K. A.,
950 Marriner, A., R.J., L., LaRoche, J., Aмоса, P., van Kooten, M., Feng, Y.-Y., Rowden,
951 A. A., and Summerfield, T. C.: Predicting changes in plankton biodiversity &



952 productivity of the EEZ in response to climate change induced ocean acidification,
953 Ministry for Primary Industrie, Wellington, New Zealand, 200, 2014.

954 Lawrence, C., and Menden-Deuer, S.: Drivers of protistan grazing pressure: seasonal
955 signals of plankton community composition and environmental conditions, Marine
956 Ecology Progress Series, 459, 39-52, 2012.

957 Le Quéré, C., Rödenbeck, C., Buitenhuis, E. T., Conway, T. J., Langenfelds, R.,
958 Gomez, A., Labuschagne, C., Ramonet, M., Nakazawa, T., Metz, N., Gillett, N., and
959 Heimann, M.: Saturation of the Southern Ocean CO₂ sink due to recent climate change,
960 Science, 316, 1735-1738, 10.1126/science.1136188, 2007.

961 Malinverno, E., Triantaphyllou, M. V., and Dimiza, M. D.: Coccolithophore assemblage
962 distribution along a temperate to polar gradient in the West Pacific sector of the
963 Southern Ocean (January 2005), Micropaleontology, 61, 489–506, 2015.

964 McIntyre, A., and Bé, A. W. H.: Modern coccolithophoridae of the Atlantic Ocean—I.
965 Placoliths and cyrtoliths, Deep Sea Research and Oceanographic Abstracts, 14, 561-
966 597, [https://doi.org/10.1016/0011-7471\(67\)90065-4](https://doi.org/10.1016/0011-7471(67)90065-4), 1967.

967 McNeil, B. I., and Matear, R. J.: Southern Ocean acidification: A tipping point at 450-
968 ppm atmospheric CO₂, Proceedings of the National Academy of Sciences, 105, 18860-
969 18864, 2008.

970 Medlin, L. K., Lange, M., and Baumann, M. E. M.: Genetic differentiation among three
971 colony-forming species of Phaeocystis: further evidence for the phylogeny of the
972 Prymnesiophyta, Phycologia, 33, 199-212, 10.2216/i0031-8884-33-3-199.1, 1994.

973 Meyer, J., and Riebesell, U.: Reviews and Syntheses: Responses of coccolithophores to
974 ocean acidification: a meta-analysis, Biogeosciences (BG), 12, 1671-1682, 2015.

975 Moy, A. D., Howard, W. R., Bray, S. G., and Trull, T. W.: Reduced calcification in
976 modern Southern Ocean planktonic foraminifera, Nature Geosci, 2, 276-280,
977 http://www.nature.com/ngeo/journal/v2/n4/suppinfo/ngeo460_S1.html, 2009.

978 Müller, M. N., Trull, T. W., and Hallegraeff, G. M.: Differing responses of three
979 Southern Ocean *Emiliania huxleyi* ecotypes to changing seawater carbonate chemistry,
980 Marine Ecology Progress Series, 531, 81-90, 2015.

981 Nodder, S. D., Chiswell, S. M., and Northcote, L. C.: Annual cycles of deep-ocean
982 biogeochemical export fluxes in subtropical and subantarctic waters, southwest Pacific
983 Ocean, Journal of Geophysical Research: Oceans, n/a-n/a, 10.1002/2015JC011243,
984 2016.



- 985 Northcote, L. C., and Neil, H. L.: Seasonal variations in foraminiferal flux in the
986 Southern Ocean, Campbell Plateau, New Zealand, *Marine Micropaleontology*, 56, 122–
987 137, 2005.
- 988 O’Dea, S. A., Gibbs, S. J., Bown, P. R., Young, J. R., Poulton, A. J., Newsam, C., and
989 Wilson, P. A.: Coccolithophore calcification response to past ocean acidification and
990 climate change, *Nature Communications*, 5, 5363, 10.1038/ncomms6363
991 <https://www.nature.com/articles/ncomms6363#supplementary-information>, 2014.
- 992 Orsi, A. H., Whitworth Iii, T., and Nowlin Jr, W. D.: On the meridional extent and
993 fronts of the Antarctic Circumpolar Current, *Deep Sea Research Part I: Oceanographic*
994 *Research Papers*, 42, 641-673, [http://dx.doi.org/10.1016/0967-0637\(95\)00021-W](http://dx.doi.org/10.1016/0967-0637(95)00021-W), 1995.
- 995 Paasche, E.: Coccolith Formation, *Nature*, 193, 1094-1095, 10.1038/1931094b0, 1962.
- 996 Paasche, E.: A review of the coccolithophorid *Emiliana huxleyi* (Prymnesiophyceae),
997 with particular reference to growth, coccolith formation, and calcification-
998 photosynthesis interactions, *Phycologia*, 40, 503-529, 10.2216/i0031-8884-40-6-503.1,
999 2002.
- 1000 Pachauri, R. K., Allen, M. R., Barros, V. R., Broome, J., Cramer, W., Christ, R.,
1001 Church, J. A., Clarke, L., Dahe, Q., and Dasgupta, P.: Climate change 2014: synthesis
1002 report. Contribution of Working Groups I, II and III to the fifth assessment report of the
1003 Intergovernmental Panel on Climate Change, *Ipcc*, 2014.
- 1004 Passow, U., and De La Rocha, C. L.: Accumulation of mineral ballast on organic
1005 aggregates, *Global Biogeochemical Cycles*, 20, GB1013, 10.1029/2005GB002579,
1006 2006.
- 1007 Patarnello, T., Bargelloni, L., Varotto, V., and Battaglia, B.: Krill evolution and the
1008 Antarctic ocean currents: evidence of vicariant speciation as inferred by molecular data,
1009 *Marine Biology*, 126, 603-608, 10.1007/bf00351327, 1996.
- 1010 Patil, S. M., Mohan, R., Shetye, S. S., Gazi, S., Baumann, K.-H., and Jafar, S.:
1011 Biogeographic distribution of extant Coccolithophores in the Indian sector of the
1012 Southern Ocean, *Marine Micropaleontology*, 137, 16-30,
1013 <https://doi.org/10.1016/j.marmicro.2017.08.002>, 2017.
- 1014 Poulton, A. J., Charalampopoulou, A., Young, J. R., Tarran, G. A., Lucas, M. I., and
1015 Quartly, G. D.: Coccolithophore dynamics in non-bloom conditions during late
1016 summer in the central Iceland Basin (July-August 2007), *Limnology and*
1017 *Oceanography*, 55, 1601-1613, 10.4319/lo.2010.55.4.1601, 2010.



- 1018 Poulton, A. J., Young, J. R., Bates, N. R., and Balch, W. M.: Biometry of detached
1019 *Emiliania huxleyi* coccoliths along the Patagonian Shelf, Marine Ecology Progress
1020 Series, 443, 1-17, 2011.
- 1021 Poulton, A. J., Painter, S. C., Young, J. R., Bates, N. R., Bowler, B., Drapeau, D.,
1022 Lyczsckowski, E., and Balch, W. M.: The 2008 *Emiliania huxleyi* bloom along the
1023 Patagonian Shelf: Ecology, biogeochemistry, and cellular calcification, Global
1024 Biogeochemical Cycles, 27, 1023-1033, [10.1002/2013gb004641](https://doi.org/10.1002/2013gb004641), 2013.
- 1025 Probert, I., and Houdan, A.: The laboratory culture of coccolithophores, in:
1026 Coccolithophores, Springer, 217-249, 2004.
- 1027 Quéguiner, B.: Iron fertilization and the structure of planktonic communities in high
1028 nutrient regions of the Southern Ocean, Deep Sea Research Part II: Topical Studies in
1029 Oceanography, 90, 43-54, <http://dx.doi.org/10.1016/j.dsr2.2012.07.024>, 2013.
- 1030 Quéré, C. L., Harrison, S. P., Colin Prentice, I., Buitenhuis, E. T., Aumont, O., Bopp,
1031 L., Claustre, H., Cotrim Da Cunha, L., Geider, R., Giraud, X., Klaas, C., Kohfeld, K. E.,
1032 Legendre, L., Manizza, M., Platt, T., Rivkin, R. B., Sathyendranath, S., Uitz, J., Watson,
1033 A. J., and Wolf-Gladrow, D.: Ecosystem dynamics based on plankton functional types
1034 for global ocean biogeochemistry models, Global Change Biology, 11, 2016-2040,
1035 [10.1111/j.1365-2486.2005.1004.x](https://doi.org/10.1111/j.1365-2486.2005.1004.x), 2005.
- 1036 Rigual-Hernández, A. S., Trull, T. W., Bray, S. G., Closset, I., and Armand, L. K.:
1037 Seasonal dynamics in diatom and particulate export fluxes to the deep sea in the
1038 Australian sector of the southern Antarctic Zone, Journal of Marine Systems, 142, 62-
1039 74, <http://dx.doi.org/10.1016/j.jmarsys.2014.10.002>, 2015a.
- 1040 Rigual-Hernández, A. S., Trull, T. W., Bray, S. G., Cortina, A., and Armand, L. K.:
1041 Latitudinal and temporal distributions of diatom populations in the pelagic waters of the
1042 Subantarctic and Polar Frontal Zones of the Southern Ocean and their role in the
1043 biological pump, Biogeosciences 12, 8615-8690, [10.5194/bg-12-8615-2015](https://doi.org/10.5194/bg-12-8615-2015), 2015b.
- 1044 Rigual-Hernández, A. S., Pilskaln, C. H., Cortina, A., Abrantes, F., and Armand, L. K.:
1045 Diatom species fluxes in the seasonally ice-covered Antarctic Zone: New data from
1046 offshore Prydz Bay and comparison with other regions from the eastern Antarctic and
1047 western Pacific sectors of the Southern Ocean, Deep Sea Research Part II: Topical
1048 Studies in Oceanography, <https://doi.org/10.1016/j.dsr2.2018.06.005>, 2018.
- 1049 Rigual Hernández, A. S., Flores, J. A., Sierro, F. J., Fuertes, M. A., Cros, L., and Trull,
1050 T. W.: Coccolithophore populations and their contribution to carbonate export during an



- 1051 annual cycle in the Australian sector of the Antarctic Zone, *Biogeosciences* 2017, 1-40,
1052 10.5194/bg-2017-523, 2018.
- 1053 Rintoul, S. R., and Trull, T. W.: Seasonal evolution of the mixed layer in the
1054 Subantarctic zone south of Australia, *Journal of Geophysical Research: Oceans*, 106,
1055 31447-31462, 10.1029/2000JC000329, 2001.
- 1056 Rintoul, S. R., Sparrow, M., Meredith, M. P., Wadley, V., Speer, K., Hofmann, E.,
1057 Summerhayes, C., Urban, E., Bellerby, R., and Ackley, S.: The Southern Ocean
1058 observing system: initial science and implementation strategy, *Scientific Committee on*
1059 *Antarctic Research*, 2012.
- 1060 Rintoul, S. R., Chown, S. L., DeConto, R. M., England, M. H., Fricker, H. A., Masson-
1061 Delmotte, V., Naish, T. R., Siebert, M. J., and Xavier, J. C.: Choosing the future of
1062 Antarctica, *Nature*, 558, 233-241, 10.1038/s41586-018-0173-4, 2018.
- 1063 Rivero-Calle, S., Gnanadesikan, A., Del Castillo, C. E., Balch, W. M., and Guikema, S.
1064 D.: Multidecadal increase in North Atlantic coccolithophores and the potential role of
1065 rising CO₂, *Science*, 350, 1533-1537, 10.1126/science.aaa8026, 2015.
- 1066 Rost, B., and Riebesell, U.: Coccolithophores and the biological pump: responses to
1067 environmental changes, in: *Coccolithophores: From Molecular Processes to Global*
1068 *Impact*, edited by: Thierstein, H. R., and Young, J. R., Springer Berlin Heidelberg,
1069 Berlin, Heidelberg, 99-125, 2004.
- 1070 Rousseaux, C. S., and Gregg, W. W.: Recent decadal trends in global phytoplankton
1071 composition, *Global Biogeochemical Cycles*, 29, 1674-1688, 2015.
- 1072 Saavedra-Pellitero, M., Baumann, K.-H., Flores, J.-A., and Gersonde, R.:
1073 Biogeographic distribution of living coccolithophores in the Pacific sector of the
1074 Southern Ocean, *Marine Micropaleontology*, 109, 1-20, 2014.
- 1075 Saavedra-Pellitero, M., and Baumann, K.-H.: Comparison of living and surface
1076 sediment coccolithophore assemblages in the Pacific sector of the Southern Ocean,
1077 *Micropaleontology*, 61, 507-520, 2015.
- 1078 Sabine, C. L., Feely, R. A., Gruber, N., Key, R. M., Lee, K., Bullister, J. L.,
1079 Wanninkhof, R., Wong, C. S., Wallace, D. W. R., Tilbrook, B., Millero, F. J., Peng, T.-
1080 H., Kozyr, A., Ono, T., and Rios, A. F.: The Oceanic Sink for Anthropogenic CO₂,
1081 *Science*, 305, 367-371, 10.1126/science.1097403, 2004.
- 1082 Salter, I., Schiebel, R., Ziveri, P., Movellan, A., Lampitt, R., and Wolff, G. A.:
1083 Carbonate counter pump stimulated by natural iron fertilization in the Polar Frontal
1084 Zone, *Nature Geosci*, 7, 885-889, 10.1038/ngeo2285



- 1085 <http://www.nature.com/ngeo/journal/v7/n12/abs/ngeo2285.html#supplementary->
1086 [information](#), 2014.
- 1087 Samtleben, C., and Bickert, T.: Coccoliths in sediment traps from the Norwegian Sea,
1088 *Marine Micropaleontology*, 16, 39-64, [https://doi.org/10.1016/0377-8398\(90\)90028-K](https://doi.org/10.1016/0377-8398(90)90028-K),
1089 1990.
- 1090 Schiebel, R., and Hemleben, C.: *Planktic foraminifers in the modern ocean*, Springer,
1091 2017.
- 1092 Schiebel, R., Spielhagen, R. F., Garnier, J., Hagemann, J., Howa, H., Jentzen, A.,
1093 Martínez-García, A., Meilland, J., Michel, E., Repschläger, J., Salter, I., Yamasaki, M.,
1094 and Haug, G.: Modern planktic foraminifers in the high-latitude ocean, *Marine*
1095 *Micropaleontology*, 136, 1-13, <https://doi.org/10.1016/j.marmicro.2017.08.004>, 2017.
- 1096 Shadwick, E. H., Trull, T. W., Thomas, H., and Gibson, J. A. E.: Vulnerability of Polar
1097 Oceans to Anthropogenic Acidification: Comparison of Arctic and Antarctic Seasonal
1098 Cycles, *Scientific Reports*, 3, 2339, 10.1038/srep02339, 2013.
- 1099 Sinha, B., Buitenhuis, E. T., Quéré, C. L., and Anderson, T. R.: Comparison of the
1100 emergent behavior of a complex ecosystem model in two ocean general circulation
1101 models, *Progress in Oceanography*, 84, 204-224,
1102 <https://doi.org/10.1016/j.pocean.2009.10.003>, 2010.
- 1103 Sloyan, B. M., and Rintoul, S. R.: Circulation, Renewal, and Modification of Antarctic
1104 Mode and Intermediate Water, *Journal of Physical Oceanography*, 31, 1005-1030,
1105 10.1175/1520-0485(2001)031<1005:cramoa>2.0.co;2, 2001a.
- 1106 Sloyan, B. M., and Rintoul, S. R.: The Southern Ocean Limb of the Global Deep
1107 Overturning Circulation, *Journal of Physical Oceanography*, 31, 143-173,
1108 10.1175/1520-0485(2001)031<0143:TSOLOT>2.0.CO;2, 2001b.
- 1109 Sokolov, S., and Rintoul, S. R.: Circumpolar structure and distribution of the Antarctic
1110 Circumpolar Current fronts: 2. Variability and relationship to sea surface height, *Journal*
1111 *of Geophysical Research: Oceans*, 114, C11019, 10.1029/2008JC005248, 2009.
- 1112 Thornhill, D. J., Mahon, A. R., Norenburg, J. L., and Halanych, K. M.: Open-ocean
1113 barriers to dispersal: a test case with the Antarctic Polar Front and the ribbon worm
1114 *Parborlasia corrugatus* (Nemertea: Lineidae), *Molecular Ecology*, 17, 5104-5117,
1115 10.1111/j.1365-294X.2008.03970.x, 2008.
- 1116 Trull, T. W., Bray, S. G., Manganini, S. J., Honjo, S., and François, R.: Moored
1117 sediment trap measurements of carbon export in the Subantarctic and Polar Frontal



1118 zones of the Southern Ocean, south of Australia, *Journal of Geophysical Research:*
1119 *Oceans*, 106, 31489-31509, 10.1029/2000JC000308, 2001.

1120 Trull, T. W., Schulz, E., Bray, S. G., Pender, L., McLaughlan, D., Tilbrook, B.,
1121 Rosenberg, M., and Lynch, T.: The Australian Integrated Marine Observing System
1122 Southern Ocean Time Series facility, *OCEANS 2010 IEEE - Sydney*, 2010, 1-7,
1123 Trull, T. W., Passmore, A., Davies, D. M., Smit, T., Berry, K., and Tilbrook, B.: The
1124 distribution of pelagic biogenic carbonates in the Southern Ocean south of Australia: a
1125 baseline for ocean acidification impact assessment, *Biogeosciences*, in press, 2018.

1126 Tyrrell, T., and Merico, A.: *Emiliania huxleyi*: bloom observations and the conditions
1127 that induce them, in: *Coccolithophores*, Springer, 75-97, 2004.

1128 Volk, T., and Hoffert, M. I.: Ocean Carbon Pumps: Analysis of Relative Strengths and
1129 Efficiencies in Ocean-Driven Atmospheric CO₂ Changes, in: *The Carbon Cycle and*
1130 *Atmospheric CO₂: Natural Variations Archean to Present*, 99-110, 1985.

1131 Winter, A., Henderiks, J., Beaufort, L., Rickaby, R. E., and Brown, C. W.: Poleward
1132 expansion of the coccolithophore *Emiliania huxleyi*, *Journal of Plankton Research*, 36,
1133 316-325, 2014.

1134 Young, J., Geisen, M., Cross, L., Kleijne, A., Sprengel, C., Probert, I., and Østergaard,
1135 J.: A guide to extant coccolithophore taxonomy, *Journal of Nanoplankton Research*
1136 *Special Issue 1*, International Nannoplankton Association, 2003.

1137 Young, J. R.: The description and analysis of coccolith structure, *Nannoplankton*
1138 *Research*. Hamrsmid B, Young JR (eds) ZPZ, Knihovnica, 35-71, 1992.

1139 Young, J. R., Davis, S. A., Bown, P. R., and Mann, S.: Coccolith Ultrastructure and
1140 Biomineralisation, *Journal of Structural Biology*, 126, 195-215,
1141 <https://doi.org/10.1006/jsbi.1999.4132>, 1999.

1142 Young, J. R., and Ziveri, P.: Calculation of coccolith volume and its use in calibration of
1143 carbonate flux estimates, *Deep Sea Research Part II: Topical Studies in Oceanography*,
1144 47, 1679-1700, [http://dx.doi.org/10.1016/S0967-0645\(00\)00003-5](http://dx.doi.org/10.1016/S0967-0645(00)00003-5), 2000.

1145 Nannotax3 website: <http://www.mikrotax.org/Nannotax3> access: July 2019, 2019.

1146 Ziveri, P., Broerse, A. T. C., van Hinte, J. E., Westbroek, P., and Honjo, S.: The fate of
1147 coccoliths at 48°N 21°W, Northeastern Atlantic, *Deep Sea Research Part II: Topical*
1148 *Studies in Oceanography*, 47, 1853-1875, [http://dx.doi.org/10.1016/S0967-](http://dx.doi.org/10.1016/S0967-0645(00)00009-6)
1149 [0645\(00\)00009-6](http://dx.doi.org/10.1016/S0967-0645(00)00009-6), 2000.

1150 Ziveri, P., de Bernardi, B., Baumann, K.-H., Stoll, H. M., and Mortyn, P. G.: Sinking of
1151 coccolith carbonate and potential contribution to organic carbon ballasting in the deep



- 1152 ocean, Deep Sea Research Part II: Topical Studies in Oceanography, 54, 659-675,
1153 <http://dx.doi.org/10.1016/j.dsr2.2007.01.006>, 2007.
1154